The effect of inversion tectonics on the Late Miocene sedimentary system in the western Pannonian Basin, Hungary:

A study based on seismic interpretation

Youri Kickken

Master thesis, Utrecht University, April 2017

Supervisors:

dr. Liviu Matenco

Attila Balázs

Abstract

The Pannonian Basin of Central Europe, a Cenozoic back-arc basin enclosed between the Alps, Dinarides and Carpathians, underwent several stages of extension and inversion. The uplift of the surrounding mountains, at the earliest Late Miocene, led to the birth of Lake Pannon. Large rivers transported sediments into this isolated lake. Particularly, the paleo-Danube and paleo-Tisza progressively filled the lake dominantly from the northern margins. Previous studies have indicated that the timing of the shelf progradation ranged between ~10-4 Ma from NW to SE. However, the link between tectonic inversion and the sedimentary infill of the basin is much less understood. In this study I used a combination of seismic and well data interpretation and cross-section reconstruction coupled to a palaeobathymetric dataset. My reconstruction quantifies the considerable thickness differences in the palaeobathymetric evolution between the paleo-highs and deep depocentres. The effects of external and internal tectonic and sedimentary forcing factors on the height of the prograding shelf-margin slope have been compared and analyzed. The climatic control is believed to have minor impact on these variations; only lake level rise is observed of max ~100 m. No major drops in lake level have been observed, as any indications of incision or erosion of the shelf are absent. Other forcing factors as the existing paleo-relief, differential compaction and syn-sedimentary tectonics (subsidence and uplift) play a major role on the temporal and spatial variations of the palaeobathymetry. The late stage inversion had a major influence on the overall sedimentary transport system, as the uplift created barriers between confined basins, resulting in sediment ponding and subsequently sediment starvation behind these highs. The proposed tectonic and sedimentary evolutionary model based on seismic and well data interpretation of the Pannonian Basin can be applied in similar inverted extensional basins as well.

Utrecht University

Table of Contents

Introduction

The Pannonian Basin is a continental back-arc basin. It is surrounded by orogens, such as the Alps, Carpathians and Dinarides (Fig. 1). The formation and extension of this back-arc basin was initiated in the latest Oligocene to earliest Miocene (~28-19 Ma). The collision between Adria and the European continent was coupled with E-directed extensional collapse, accommodated by fast rollback of the Carpathian slab (e.g. Ratschbacher et al., 1991; Horváth et al., 2015). This eastward extension resulted in lithospheric thinning and the opening of a series of half-grabens. The relatively short time interval of basin formation and deformation is characterized by multiple phases of extension and episodes of basin inversion (Fig. 2). The overall pattern of tectonic phases in the Pannonian Basin is characterized by a sequence of four substantial events. The first phase is the syn-rift extension during the Early and Middle Miocene. This is followed by the first phase of inversion during the latest Middle to early Late Miocene. The uplift of mountain belts around the Pannonian Basin resulted in a, widely accepted, unconformity (Base Pannonian unconformity) characterized by angular discordance and erosional hiatus in centermost areas of the basin (Horváth et al., 2015).
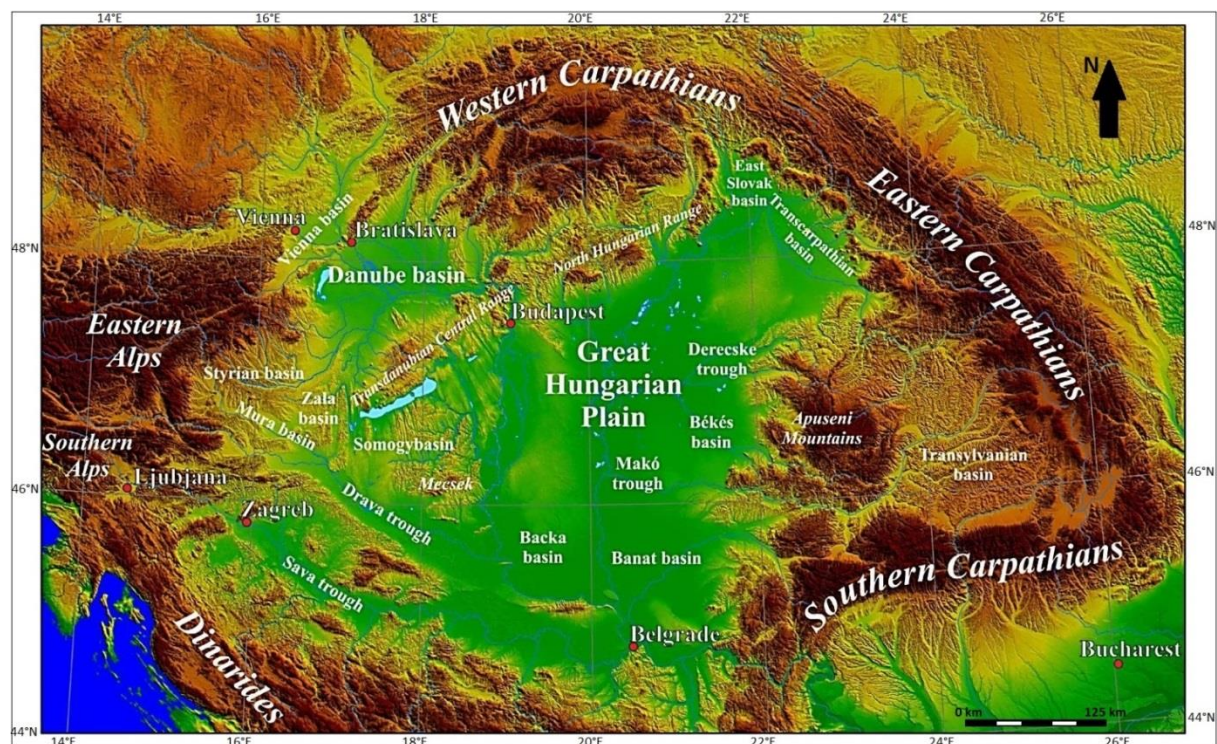

Figure 1: Terrain model of the Pannonian Basin showing its position within the Alpine-Carpathian-Dinaric mountain belt (modified after Horváth et al., 2015). Moreover, the locations of several different subunits are indicated.

The next phase during the Late Miocene is characterized by thermal subsidence and is considered to be the onset of the post-rift phase (Horváth et al., 2015). However, this boundary seems to be diachronous throughout the Pannonian Basin and can be interpreted between ca. 12-9 Ma (e.g. Tari et al., 1999; Matenco and Radivojevic, 2012). The last and still ongoing neotectonic phase is characterized by compression, inversion of earlier structures via strike-slip faulting and lithospheric folding (Bada et al., 2007). The most common style of neotectonic deformation is the positive inversion of earlier syn- to post-rift faults and associated seismicity (e.g., Bada et al., 2007, Fodor et al., 2005). Resulting structures as consequence of this inversion influenced the overall sedimentary architecture and transport routes in the basin (e.g., Uhrin et al., 2009).
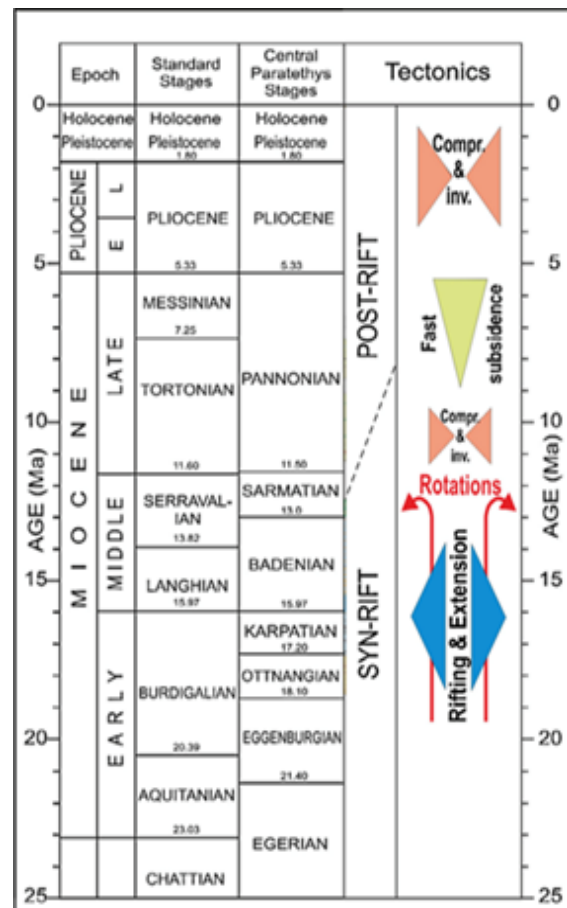
Figure 2: Chart summarizing the main tectonic phases during the Miocene - Quaternary (modified after Horváth et al., 2015).

The uplift of the mountain belts surrounding the Pannonian Basin, led to its separation from the remainder of the Paratethys, from the Late Miocene. This led to the birth of Lake Pannon, a large isolated lake with a lifetime of ~8 Myrs (Magyar et al., 2013). Influx of sediments was transported by rivers, during the post rift phase, particularly the paleo-Danube and paleo-Tisza progressively filled up the lake from the north towards the south and a reasonable timing of the shelf edge progradation has been elaborated, ranging between ~10-4 Ma (Fig. 3, Magyar et al., 2013). Minor sediment flux derived from the southern basin margins (e.g. ter Borgh, 2015).
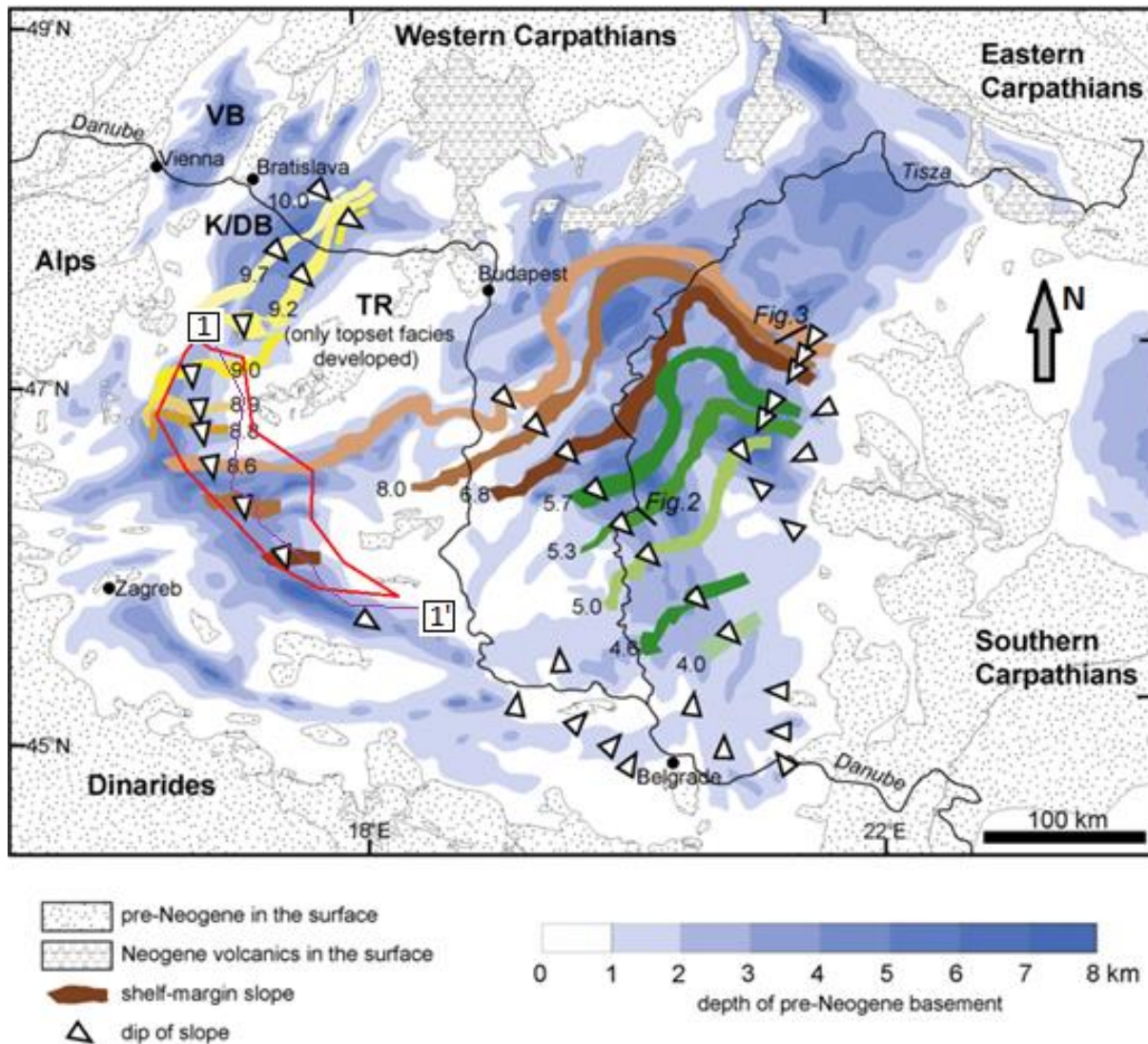
Figure 3: Map showing the progradation of the shelf-margin slopes of the paleo-Danube and the paleo-Tisza (Modified after Magyar et al., 2013). The red box indicates the research area that is covered in this project. The northern part of the area consists of the western margin of the Transdanubian Central Range, the Zala- and Mura basins. In the southern direction, the area consists of the Drava Through and the western part of the Somogybasin. The southernmost tip of the area terminates at the western boundary of the Backa basin. For locations of different subunits, see Fig. 1. The bypass of the Late Miocene prograding delta front through the northern part of the area is estimated to have occurred ~9 Ma (e.g. Magyar et al., 2013; Vakarcs et al., 1994), whereas it happened in the southern part during late Pannonian times (~6 Ma). The purple line indicates the location of the cross-section shown in Fig.6. Abbreviations: TR Transdanubian Central Range; VB: Vienna Basin.

The objective of this research is to quantitatively analyze the inversion related structures in the SW part of the Pannonian Basin (Fig. 3) and its influence on the basin fill, with special interest on the prograding shelf-margin slope and the paleo-water depth of Lake Pannon.

The analysis contains an accurate depth conversion of the main interpreted horizons, which could be used as the input data for the reconstruction. This is followed by precise decompaction of the Neogene sediments based on available well data.

As a result of the balanced cross-section by the MOVE reconstruction a precise palaeobathymetric dataset can be obtained from the height of the prograding shelf-margin slopes.

The described methodology will be used to investigate, which seismic facies and associated sediments comprise the prograding sequence. Moreover, the effects of different forcing factors such as differential compaction, syn-sedimentary tectonics (subsidence and uplift) and the presence of a paleo-relief at the onset of Pannonian times are constrained. Furthermore, the possibility of an estimation of shortening as a consequence of neotectonic folding is investigated.

The tectonic history leading to the formation of the Pannonian Basin

In the following paragraph the geological history of the Pannonian Basin will be elaborated by dividing the evolution into three major phases. The pre-rift evolution of the area is elaborated from the Early Cretaceous to Paleogene. The subsequent extensional phase during the Early to Middle and earliest Late Miocene is discussed. Finally, the neotectonic phase during the Latest Miocene to Holocene is elaborated.

Pre-rift evolution of the area

The actual formation of the Pannonian Basin during the Miocene to Quaternary was proceeded by a pre-Neogene orogenic evolution that resulted from the opening and subsequent closure of two different oceanic realms (Balázs et al., 2016). The oceanic realms: the Triassic-Cretaceous Neotethys and the Middle-Jurassic-Tertiary Alpine Tethys separated three different continental units (Handy et al., 2013; Horvath et al., 2015; Schmid et al., 2008). In the NW, the ALCAPA mega unit can be seen as the purple structure (Fig. 4). This mega unit is an Adriatic-derived block that was sutured to Europe during the northward Cretaceous-Eocene closure of the Alpine Tethys (Schmid et al., 2008). Moreover, the Dacia mega unit to the E and SE, indicated with orange (Fig. 4). The Dacia unit separated from Europe during the late Jurassic opening of the Cehlau-Severin Ocean (Schmid et al., 2008). Finally, the Tisza mega unit in the South, indicated in light blue (Fig. 4), drifted away from Europe during Middle Jurassic and sutured together with the Dacia unit during the late Jurassic late-Early Cretaceous as consequence of the closure of a NE branch of the Neotethys Ocean (Schmid et al., 2008 and references therein). The final closure of the Neotethys Ocean by subduction and collision in latest Cretaceous-Eocene times has juxtaposed the Tisza-Dacia upper tectonic plate with the lower Dinaridic unit, the latter being built up by thick skinned thrust sheets deforming the former Adriatic continental margin (Schmid et al., 2008 and Balázs et al., 2016).

These kinematics coupled with the Neogene formation of the Pannonian Basin has created a large amount of translations and opposite sense rotations accompanying the extension of these continental units (Balla, 1987). For ALCAPA this meant a counterclockwise and for the Tisza-Dacia mega unit a clockwise rotation. The two mega-units were juxtaposed along a major suture zone also known as the Mid-Hungarian Fault zone. This zone possibly accommodated the change in polarity from the southward subduction of the Alpine Tethys in the Alps-Carpathians to the northward subduction of the Neotethys in the Dinarides (e.g. Csontos and Nagymarosy, 1998; Schmid et al., 2008).
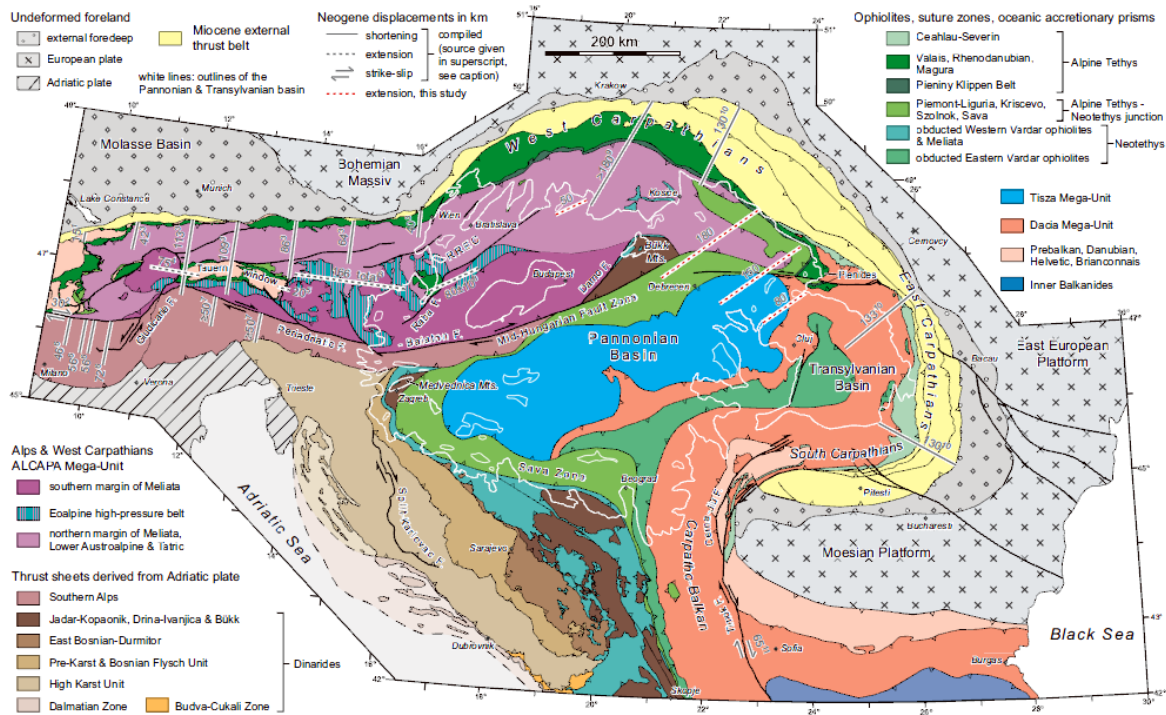
Figure 5: Tectonic map of the Alps, Dinarides and Carpathians. This map can serve as a base for the Early Miocene restoration of the Pannonian Basin formation. Abbreviations: Mts. = Mountians, RREC = Raba River extensional corridor, F. = Faults. Geographic names are given in italics (Ustaszewski et al., 2008).
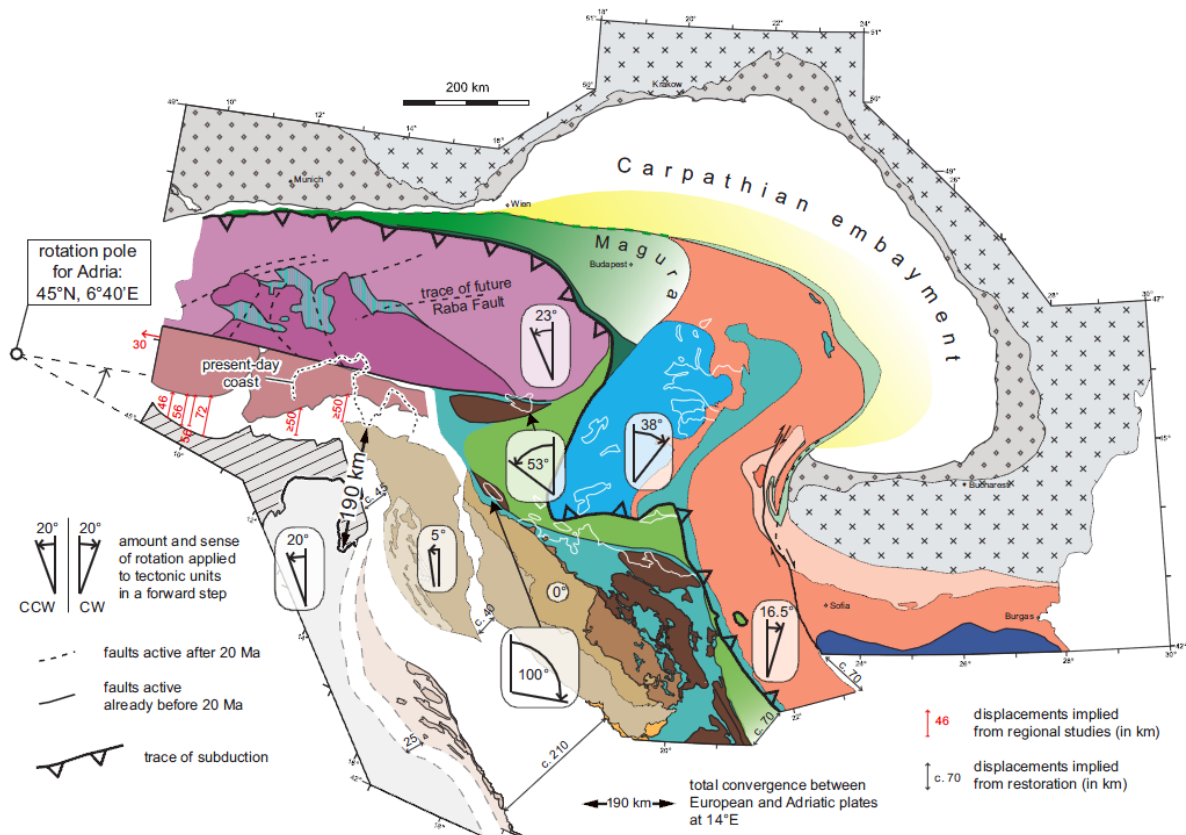
Figure 4: Schematic overview of the tectonic units in the Alps, Dinarides and Carpathians for the Early Miocene. Colours and patterns of the tectonic units correspond with the legend of figure 4 (Ustaszewski et al., 2008).

9

The Pannonian Basin formation (syn-rift phase)

Miocene extension resulted in the actual formation of the Pannonian Basin. The exact dating of the onset of extension is a matter of debate. However, extension that led to the formation of the Pannonian Basin is traditionally dated as latest Oligocene, earliest Miocene (~28-19 Ma). Horváth et al. (2006) summarizes the formation of the Pannonian Basin as the result of extensional collapse of an overthickened Alpine crustal block. It is considered that this thick orogenic crust was a result of nappe stacking in the Alps during the Cretaceous to Paleogene.

This built up of thick orogenic crust led to orogen-parallel extension and thinning of the crust (e.g. Cloetingh et al., 2006; Ratschbacher et al., 1989). The orogen-parallel extension is assisted by the rollback of the Carpathian slab. The rollback of the slab led to lithospheric thinning and opening of a series of half-grabens, and this accommodated the lateral extrusion of crustal blocks to the east. This is supported by Matenco and Radivojević, (2012) as they stated that the extension is related to the rapid Miocene rollback of a slab of the Carpathians and Dinarides.

A peak period of extension occurred during the late Early to Middle Miocene. This period of extension formed the main structural patterns in the basin (Fig. 6). Confining the extension and rifting phase is performed by thermochronological studies, for instance, in the Tauern window. The Tauern window is situated at the western margin of the ALCAPA mega-unit (Fig. 4). It exposes highly metamorphosed oceanic and continental thrust sheets beneath Austroalpine nappes (Horváth et al., 2015). The thermochronological studies show an increase of exhumation rates around 20-21 Ma.

During the Middle Miocene the ALCAPA and Tisza-Dacia mega-units of the Pannonian Basin became juxtaposed, along a major suture zone, the Mid Hungarian Fault Zone (Fig. 6). This wide fault zone accommodates the kinematics of clockwise (Tisza-Dacia) and counterclockwise (ALCAPA) differential rotational displacement of the mega-units.

Recent studies corroborated the opposite rotation of the two mega-units, but found differential rotations within each unit and distinct phases of rotational event, with a peak activity in the 18-10 Ma time interval (e.g. Marton and Fodor, 2003; van Hinsbergen et al., 2008; Ustaszewski et al., 2008).

Recent models agree that the peak of back-arc extension was reached during the Middle Miocene times (ca. 15-12 Ma). After the termination of subduction roll-back the extension gradually ceased during the Middle to Late Miocene (e.g., Horváth et al., 2015; Matenco et al., 2016; Merten et al., 2010; ter Borgh, 2013).
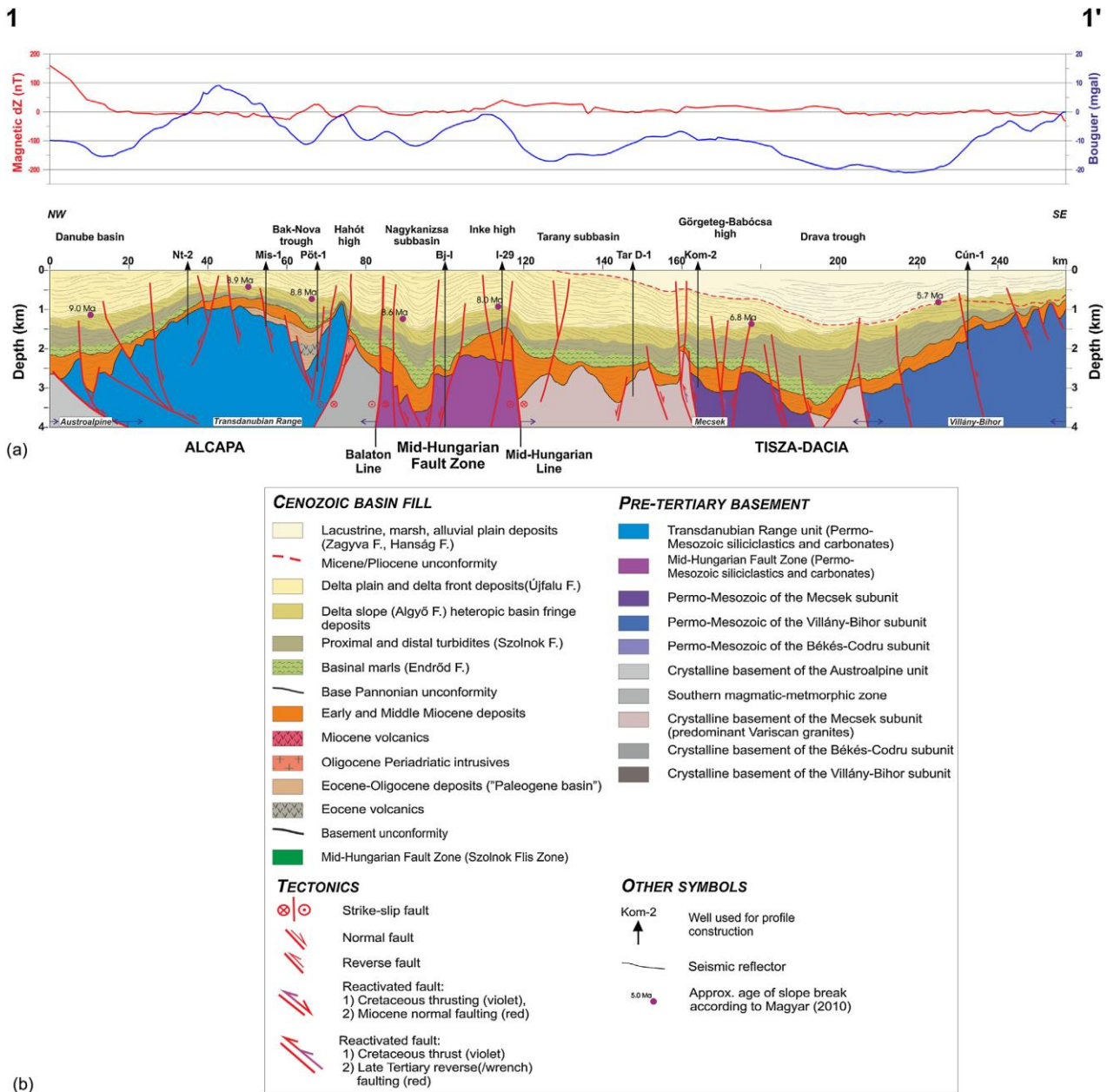
Figure 6: NW-SE orientated cross-section across the western Pannonian Basin (Horváth et al., 2015). For location, see Fig.3.

Post-extensional evolution

The syn-rift/post-rift boundary appears to be diachronous in the Pannonian Basin system (Tari et al., 1999; Balázs et al., 2016). However, in the largest part of the basin and dominantly in the Great Hungarian Plane, the onset of the post-rift phase is interpreted at ~12-9 Ma (e.g., Matenco and Radivojevic, 2012). The boundary of the Middle and Late Miocene (11.63 Ma, sensu ter Borgh et al., 2013) is a marked unconformity (Base Pannonian unconformity) which was traditionally interpreted as a general syn-rift/post-rift boundary (e.g., Horváth et al., 2006). This unconformity is associated with the peak period of collision in the East Carpathians.

A seismic interpretation study in the SE part of the basin by Matenco and Radivojevic (2012) suggests that extensional deformation was diachronous across the basin and migrated with time and in space from 28 Ma near the Dinarides to 8 Ma NE and E wards. This means that the Dinaric thrusts, formed in the Eocene and Oligocene, reactivated and formed extensional structures. The subsequent depocenter progressively shifted towards the center of the Pannonian Basin and eventually towards the east.

The first post-rift inversion of the Pannonian Basin is characterized by long-term thermal subsidence, which led to the formation and maintenance of deep basins, hosting several thousand meter thick sediments of Lake Pannon (Sztanó et al., 2013).

The basin fill recorded an initial transgression followed by shelf-margin slope progradation driven by the influx of sediments transported by rivers, during the post-rift phase, particularly the paleo-Danube and paleo-Tisza progressively filled up the lake. The shelf-margin prograded ~400km in 6 Myrs until ~4Ma from the NW and NE in a ~S-SE direction (Magyar et al., 2013; ter Borgh et al., 2015; Vakarcs et al., 1994). A reasonable timing model of this shelf edge progradation has been elaborated (Fig. 2, Magyar et al., 2013).

Gradual cessation of extension and the change towards a more compressional regime and subsequent inversion took place from the latest Miocene; this is caused by the continuing counterclockwise rotation and push of the Adriatic micro plate (Bada et al., 2007). The subsequent deformation event, which is still active, created large-scale compressional structures near the Dinaridic margin and dominantly transcurrent kinematics elsewhere (Fodor et al., 2005). The Late Miocene to Quaternary inversion is characterized by reactivation of normal faults, formation of strike-slip zones and major differential vertical movements. These inverted normal faults and its resulting structures influenced the progradation of the basin fill throughout the SW Pannonian Basin (Uhrin et al., 2009).

There are two clear unconformities observed above the Base Pannonian unconformity. The first unconformity formed at ~6.8 Ma is most probably related to either a significant absolute water level fall of Lake Pannon (e.g., Vakarcs et al., 1994), or related to cross-over zones of different progradational directions (Magyar and Sztanó, 2008).

The second unconformity is angular and locally erosional and marks the boundary between the Miocene and the Pliocene (e.g., Vakarcs et al., 1994). The unconformity has previously been mapped based on seismic onlaps onto shelf-margin clinoforms and local erosional features such as small scale channels or lateral truncations (Magyar & Sztanó, 2008; ter Borgh et al, 2015).

There are two different interpretations for the cause of this unconformity. Firstly, the interpretation that the unconformity is related to differential tectonic uplift occurring during the onset of the latest Miocene-Quaternary basin inversion, which was superposed over a long term alternation of aggradational and progradational deposition (Horvath et al., 2006; Magyar and Sztanó, 2008).

Another interpretation proposed to be responsible for this unconformity is that the inversion was accompanied by absolute lake-level fall of up to 200 m, followed by a lake level rise in concert with the Messinian Salinity Crisis (Juhász et al., 1999; Csató et al., 2013).

However, this interpretation is debated (e.g. Leever et al., 2010; Krijgsman et al., 2010). Ter Borgh (2015) states, the absolute high amplitude lake level fall of up to 200 m is unlikely as it could only be explained by a river connection of the Pannonian Basin with the Dacian basin. In this scenario an absolute fall of water level occurred in the Dacian Basin, which is in turn linked to the regional Mediterranean Sea level drop (Csato et al, 2013). Lake Pannon would then have worked as a hanging lake tempering the absolute fall of water level in the Dacian Basin. The river connection should have incised through the Southern Carpathians, the natural barrier between the two basins. Meaning that the river had to incise into bedrock. However, observing this would be difficult as the rate of a river incising into bedrock is in the same order as the thermal subsidence rate of the Pannonian Basin itself (ter Borgh, 2015).

Evolution of Pannonian Basin sedimentation

A description about the depositional environment and each stratigraphic unit (Fig. 7) is preferable in order to note the main environmental and tectonic changes during the Miocene to Quaternary. The main focus will eventually be on the sedimentary units of the prograding shelf-margin slope.

Early to Middle Miocene infill

The Early Miocene depositional environments of the Pannonian Basin are dominantly consists of continental deposits like fluvial and lacustrine (*e.g. Szászvár Formation*) sedimentary rocks (Matenco and Radiovojevic, 2012). The Szászvár Formation consists of conglomerates, sandstones and mottled clays deposited in river-to-lake environments. Lacustrine sedimentation was influenced with pyroclastics. Moreover, lakes prevailed in the upper part of these successions, but they still remained isolated until the main marine transgression, which occurred most probably during late Karpatian times (Saftić et al., 2003). Karpatian sediments in SW Hungary consist of terrestrial deposits (conglomerates, sand –and siltstones) of lakes and large alluvial fans.

Early Middle Miocene sea level rise (Saftić et al., 2003), resulted in the deposition of deep basinal sediments (*e.g. Baden and Szilágy Formations*) in the center of the extensional (half-) graben, while deposition along their margins dominated by shallow marine sedimentation (*e.g. Hidas and Rákos Formations*). The Badenian is considered as the last fully marine period in the life of the Paratethys.

Following the Sarmantian times, the structural changes in the surrounding Alpine-Carpathian mountain belt led to the final isolation and birth of Lake Pannon. This resulted in the deposition of thin-bedded calcareous marls (e.g. Tinnye and Kozárd Formations) Sarmantian deposits are found in conformable successions (Saftić et al., 2003).

Pannonian (Late Miocene to Pliocene) infill

Sediments of the Late Miocene comprise the major part of the basin-fill succession in the Pannonian Basin. As a result of the low angle normal faults and strike-slip faults formed in the Middle Miocene, a fairly heterogeneous topography had resulted by the beginning of the Late Miocene (Sztanó et al., 2015).

This relief evolved further during the post-rift inversion events. As a consequence of these late differential vertical movements the lake floor had considerable relief, consisting of both elevated basement highs and deep sub-basins in close proximity (Fig.6).

Development of the deep basins reflected by their sedimentary fills follows a uniform pattern, only their initial relief (depth) and local rates of subsidence may have been different (Sztanó et al., 2015).

Depending on the paleogeographic position, namely the tectonically determined coeval relief of the basin floor, Lake Pannon sediments either conformably overly Sarmantian layers, or they unconformably cover older sediments, or occasionally even the crystalline basement on uplifted blocks (Saftić et al., 2003).

Coeval sedimentation of the Late Miocene reflects the deposition of a number of diachronous lithostratigraphic formations that mirror the various lithofacies associations of a deep lake depositional environment throughout alluvial plain environment (Sztanó et al., 2013).
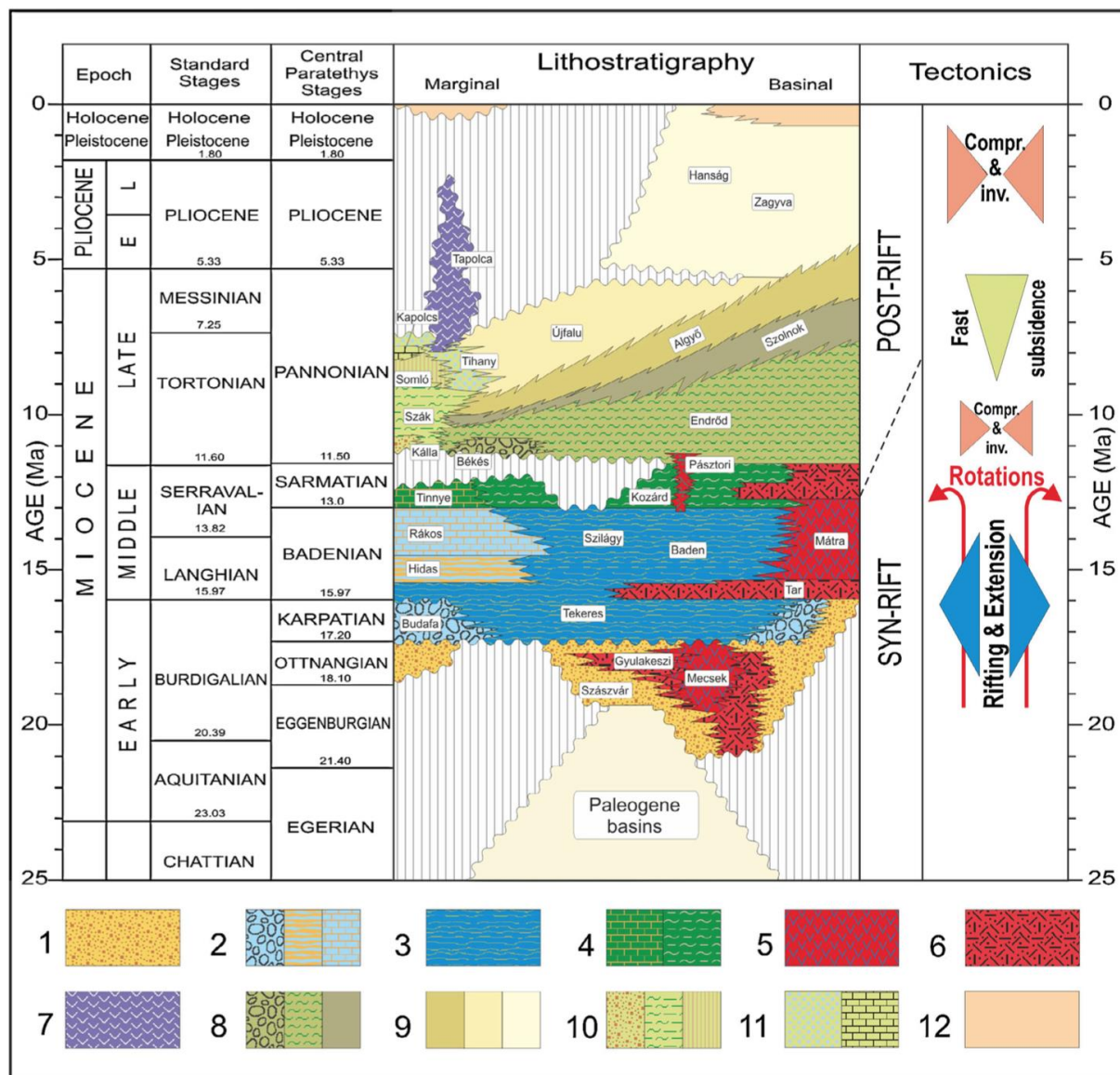
Figure 7: Stratigraphic chart showing the main syn -and postrift formations of the Pannonian Basin. The Hungarian formation names are used as the research area is located in Hungary (Horváth et al., 2015). Legend numbering: 1) Fluvial and Lacustrine; 2) Marine basin margin formations; 3) Marine pelagic; 4) Brackish basin margin; 5) Volcanics, mostly andesites; 6) Volcanics, mostly rhyolitic ignimbrites and tuffs; 7) Volcanics, alkali basalts; 8) Lacustrine, deep basin; 9) Lacustrine, shelf slope to plain; 10) Lake margin; 11) Alluvial plain; 12) Fluvial and Aeolian.

The eroded and relief rich lake floor started to subside in early Pannonian times and the rising lake level resulted in fast transgression. At ~9.8 Ma Lake Pannon reached its largest extent. This large and deep lake was characterized by a well-developed shelf system (Fig. 8) along the lake margin (Magyar et al., 1999). This shelf system was fed by a massive influx of sediments from the NW and NE. The progradation of sediments roughly follow the present Danube and Tisza river (Fig. 3), suggesting the existence of the paleo-Danube and paleo-Tisza rivers. Transdanubia and the research area more to the SW were mostly under influence of the sediments fed from the NW.

Nowadays the Danube River originates in the Black Forest in the SW part of Germany. The river crosses the North Alpine Foreland basin into the Pannonian Basin system and it eventually drains into the Black Sea. The Paleo-Danube came into existence at the beginning of the Late Miocene, about 10-11 Ma ago, when tectonic uplift of the western North Alpine Foreland Basin changed the westward-directed drainage pattern of the Alpine foreland, and a new river, originating in the central Swiss Alps, cut through the southern margin of the Bohemian Msassif to the east (Magyar et al., 2013).

The Paleo-Danube supplied sediments to Lake Pannon from the NW (Fig. 8), and the origin of these sediments lies in the Western-Carpathians and the Alps. During the early Late Miocene the Pannonian Basin was still under a phase of inversion. At this time Lake Pannon did not reach its full extent. This resulted in a delta, which reached as far as the Vienna Basin. During the Late Miocene and Early Pliocene, as fast subsidence progressed, the delta of the Paleo-Danube reached the deeper parts of the Pannonian Basin and finished near the junction between the South Carpathians and Dinarides (ter Borgh et al., 2015; Juhász et al., 2007). This resulted in thick Neogene lacustrine depositional sequences (Magyar et al., 2013).
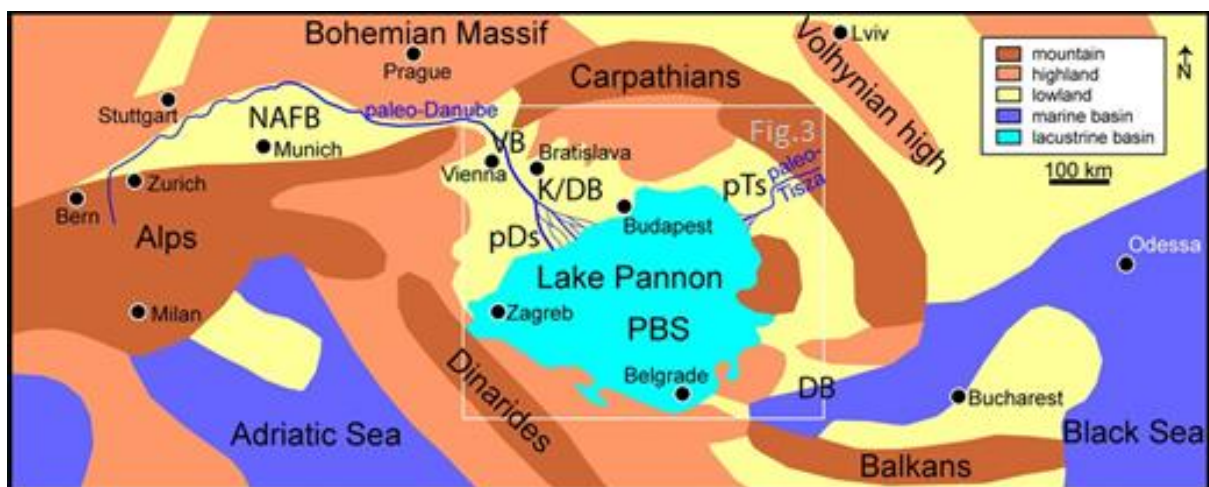

Figure 8: Schematic map showing the entire paleo-Danube river system (modified after Magyar et al., 2013).

The associated prograding shelf-margin slope filled Lake Pannon with sediments from the NW towards the south. The prograding shelf-margin slope sediments are therefore time transgressive (Fig. 9). Minor sediment flux derived from the southern basin margins (e.g., ter Borgh 2015).

The initial sediment influx was very low in comparison with the high water-level rise and this resulted in the deep hemi-pelagic deposition of the *Endrőd Formation* in the deep basins, which consists of calcareous marls and claymarls (Fig. 9, dark blue sediments). In the more marginal parts of the basin coarse grained rocks due to abrasion (*e.g. Kálla and Kisbér Formations)* are deposited.

A gradual transition from the marly *Endrőd Formation* to the turbiditic bodies of the *Szolnok Formation* originating from the slopes occurred. This *Szolnok Formation* (Fig. 9, yellow bottomsets) is built up by alternating fine-grained sandstone and pelitic layers. Upslope the foreset sediments from the *Algyő Formation* are indicated in green (Fig.9). This formation comprises mainly of silt and argillaceous marls. The heights of the prograding foresets of the Algyő Formation indicate the paleo-water depth of Lake Pannon.

Further upslope the topsets of the *Újfalu Formation* consist of coarsening-upwards sand sheets in the lower part and in the upper part fining-upwards channel sand bodies from a coastal plain environment.

The typical expression in seismic lines of these prograding shelf slope sediments provides an excellent lateral correlation of seismic facies. These diachronous associations are also correlated by magneto- and bio-stratigraphic studies calibrated by a limited number of absolute age measurements (Magyar and Sztanó, 2008; Magyar et al., 2013).
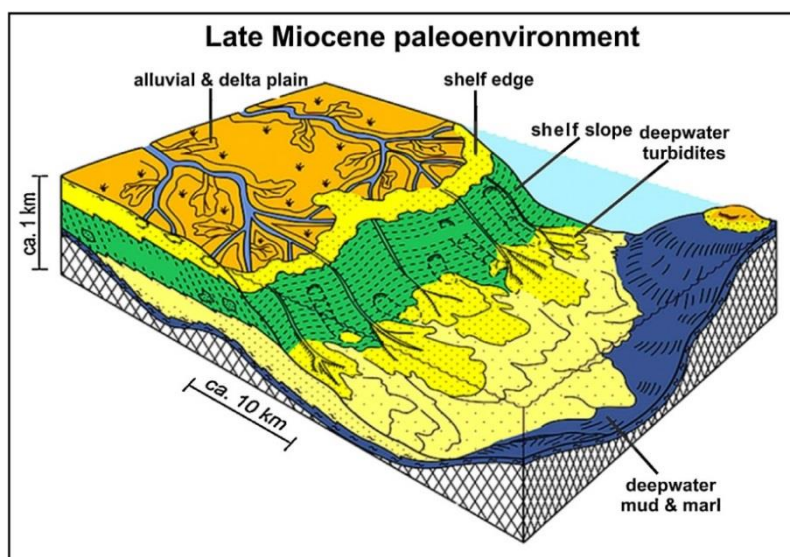
Figure 9: Schematic figure showing the prograding shelf-margin paleo-environment (Juhász et al., 1991).

Pliocene to Quaternary infill

Above these strata a cessation of lacustrine influence is found as the shelf-margin slope of Lake Pannon prograded further towards the south. The coastal plain environment was replaced by an alluvial plain across a larger and larger area (Juhász et al., 1991). This led to the channel fill, floodplain and marsh deposits of the *Zagyva and Hanság Formations*. A continuous passing into recent sediments is noticed. The thickness of Neogene and Quaternary sediments in the Pannonian Basin exceeds 7 km in the deepest troughs and the average sediment thickness is 2-3 km (Fig. 6, Drava through).

Data and Methods

The analysis performed in this project is focused on the link between tectonic structures and sedimentation in the SW part of the Pannonian Basin. The link between the subsurface neotectonic structures and the influence on the progradational shelf-margin slope is mainly based on 2D seismic interpretation via a tectono-sedimentary study. This is coupled by a cross-section reconstruction of the area, taking in consideration the compaction and porosity characteristics of the prograding shelf-margin sediments.

Seismic and Well data

The research area is located in the SW part of Hungary, close to the Hungarian-Croatian border. The area extends between 46° and 47° N and 17° and 18° E (Fig. 3 and 10) and is limited by the seismic data availability.

A dense network of 212, 2D seismic lines, divided over 17 different surveys (appendix A) is provided by the Department of Geophysics, Eötvös Loránd University. The quality of the 2D seismic lines, especially the resolution and the signal/noise ratio, decreases significantly below the Miocene sediments. The pre-Neogene interpretation of the large scale inverted faults was therefore supported by previous studies in the area. However, the main structures and sediments that are important for this research are well imaged by the seismic lines. Moreover, in this research only a limited number of seismic transects are shown, usually across the strike of the main subsurface tectonic structures.

The well data used for calibration of the seismic lines consists of 17 wells with different data composition (Table 1).

Errors related to uncertainties in data and interpretation come from mis-ties in the seismic data, wrong calibration of the velocity-depth profile and the decompaction of lithologies during the reconstruction.

Uncertainties in mis-tie calibration between intersecting seismic lines (Bishop and Nunns, 1994) range between ~20-40 m. At the start of the seismic interpretation mis-tie analysis was performed for both a vertical shift and a gain in amplitude (appendix B). The error range during time to depth conversion is between ~50-100 m. As a consequence of decompaction an error range is probably below ~100 m.

Table 1: Enumeration of well data.

Well Name	Well top data	Analog Lithological trend curve data	Shale/Sand ratio data	Time depth (checkshot) data	Directly linked to seismic line
Misefa - 1	✓				
Potrete - 1	✓				✓
Szenta -1	✓				
Somgyudvarhely - 4	✓				✓
Rinyaszentkiraly - 2	✓				✓
Komlosd -1	✓				✓
Barcs – NY1	✓	✓	✓		
Tarany - 2	✓	✓	✓		
Semjenhaza – 3	✓	✓	✓		
Felsoszentmarton - 1	✓	✓	✓		✓
Gyekenyes - 1	✓	✓	✓		✓
Darany – 1					✓
Darany – 3				✓	
Tar_D_1				✓	✓
Liszo - 1				✓	
Barcs - NY7				✓	
B-IX				✓	✓

Seismic interpretation

The seismic data is analyzed via a typical seismic interpretation methodology in the Hungarian EOV (EPSG: 23700) coordinate system (Timár and Molnár, 2002; appendix C). Firstly, defining major faults in the area in combination with reflector terminations such as: truncations, onlaps, toplaps, offlaps or downlaps. This was followed up by the interpretation of the overall subsurface structures with special interest for the Base Pannonian unconformity in the research area (Appendix D) in order to define a representative cross-section of the area.

Correlation of seismic and well data

The correlation of the seismic and well data is done by a simple seismic to well-tie methodology. The provided well tops are correlated with interpreted horizons in order to re-evaluate and correct the initial interpretation.

Cross-Section definition

The defined cross-section consists of several individual or partial seismic lines (Table 2). This cross-section (Fig. 10, red line) represents the overall geology in the area as the orientation is perpendicular (NNW-SSE) to the strike (E-W) of the major tectonic structures and parallel with the prograding (NNW-SSE) shelf-margin slope (Fig. 3). Moreover, it includes a clear definable seismic character of the prograding shelf-margin slope.

Table 2: Lateral (NS) enumeration from north to south of seismic lines.

Cross-Section
Na-69
Na-61
So-1
So-82
KAD-20
D-3-c
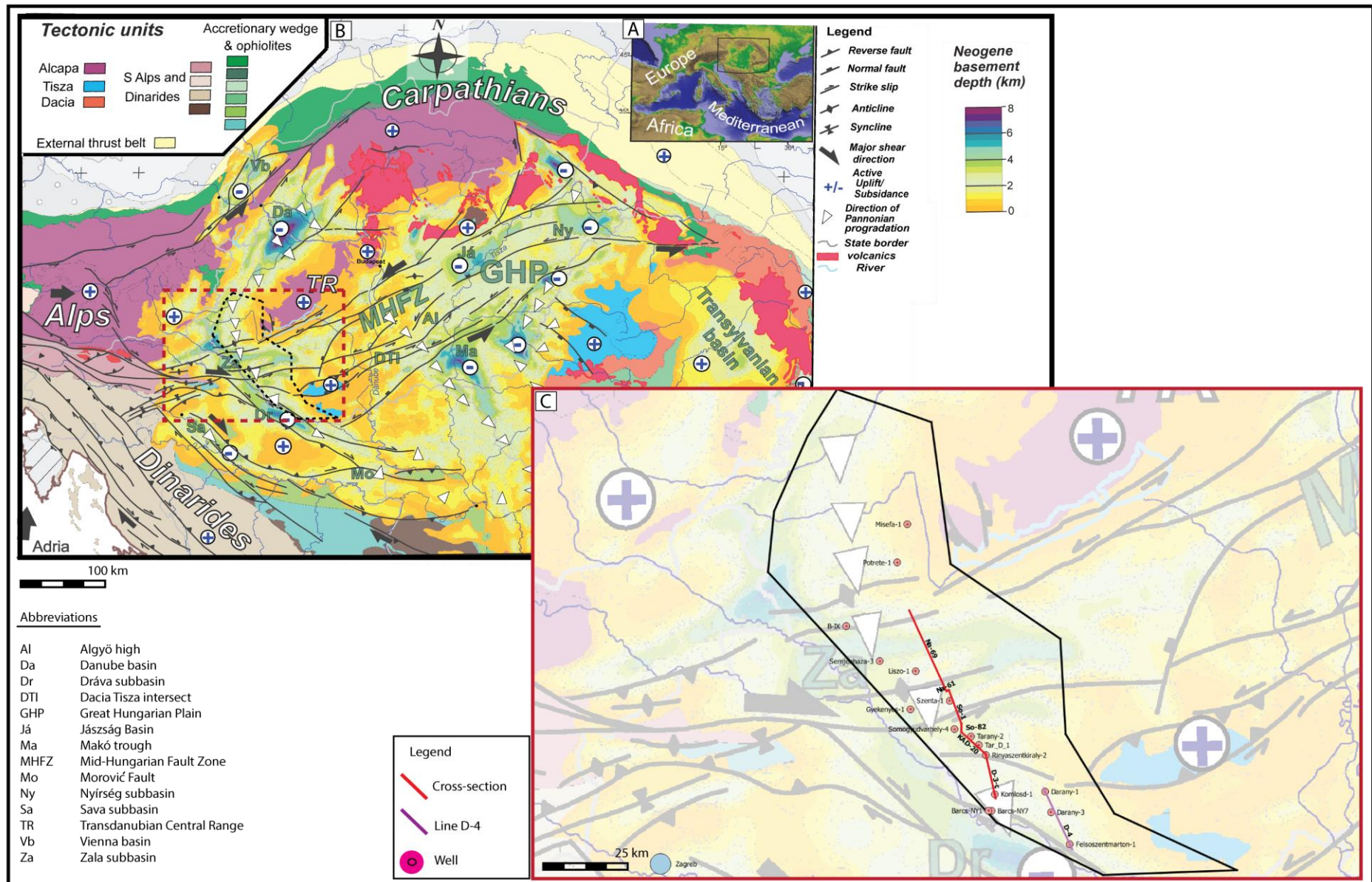
Figure 10: (A) Location of geological map. (B) Miocene-Quaternary tectonic map of the Pannonian Basin and the Alps-Carpathians-Dinarides system. Moreover, this map shows the Neogene sediment cover of the Vienna, Transylvanian and Pannonian Basins overlying the pre-Neogene basement and corresponding structures and showing the major Miocene to Quaternary faults. Finally, the directions of Pannonian progradation are shown on top (modified after Schmid et al., 2008, Bada et al., 2007, Balázs et al., 2016, Magyar et al., 2013 and Horváth et al., 2015). (C) Zoom in of the research area indicating the position of the cross-section, wells and seismic line D-4 (fig. 18).

Interpretation of the prograding shelf-margin clinoforms

The large syn-kinematic sedimentation rate of the Pannonian Basin increased the resolution of our interpretations and enabled us to locally detect a higher order sequence stratigraphic cyclicity also in the seismic data. The continuity, terminations, amplitude, frequency and distribution of reflectors define various seismic facies units, which were subsequently grouped into seismic facies associations. They are controlled by the rate of accommodation and the sediment supply (e.g. *Catuneanu et al.,* 2009 and Nichols, 2009).

The stratigraphic interpretation of the shelf-margin clinoforms follows a classical approach, but requires further explanation. The basis lies on the readily available principles of sequence stratigraphy that study the relationship between sediment supply and the available accommodation space (e.g. *Catuneanu et al.,* 2009; Nichols, 2009; Helland-Hansen and Hampson, 2009); the application to tectonically active basins is less known. In active basins, the system tracts and sequences are linked to vertical movements; they can be related to individual events of fault activation and are independent from the known cyclicity timescales of the classical sequence stratigraphy (Miall and Miall, 2001).

For this reason the methodology is simplified by dividing the seismic profile of the clinoforms (Fig. 11) into different seismic facies associations related to stratigraphic domains. These divisions result in different seismic facies related to the total system of the prograding shelf-margin slope. Essentially, this means a division of the prograding clinoform in three different zones; bottomset (Szolnok Fm.), foreset (Algyö Fm.) and shelf (Újfalu Fm.).
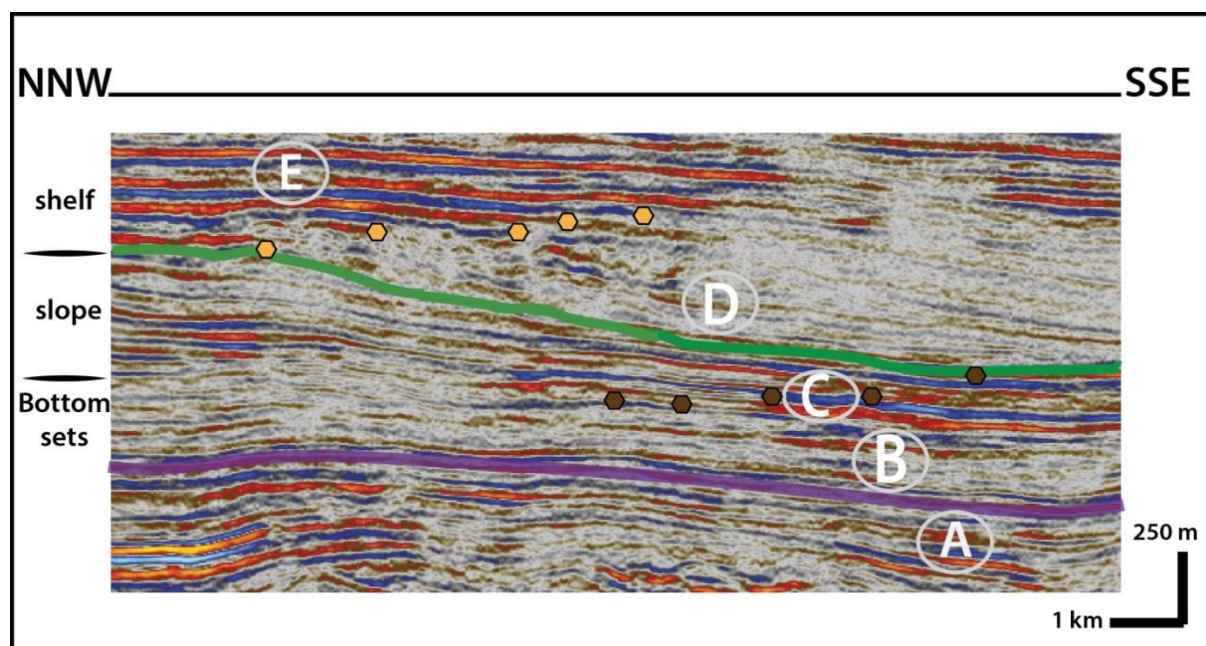
Figure 11: Part of seismic line KAD-73 showing seismic facies of the prograding and aggrading shelf-margin. The lithological units, indicated in A-E, are defined as strongly diachronous lithostratigraphic units. A: Middle Miocene, B: Endröd Fm., C: Szolnok Fm, D: Algyö Fm., E: Újfalu Fm. The green line indicates a complete interpreted clinoform (c.f. Helland-Hansen and Hampson, 2009). The clinoform line is interrupted by the shelf-edge (yellow points) and the start of the bottom sets (brown points). The Base Pannonian is indicated in purple. At the margins it is a clear unconformity and becomes a correlative conformity in the basin centers.

Porosity Analysis

Performing a porosity analysis is necessary to reconstruct the process of compaction of the Neogene to Quaternary sediments. A porosity-depth relationship for the Neogene siliciclastic sediments in the Great Hungarian plane (GHP) has been constructed by Szalay et al., 1982 (Fig.12). These curves have been updated for the western part of the Pannonian Basin by Lenkey, (1999). The curves show a different trend, which has two distinctive reasons.

The difference in source areas of the sediments between the GHP and the western part of the Pannonian Basin gives a difference of sediment grain size. At the end of the rifting phase the Pannonian Basin exhibited an uneven basin morphology. This morphology consisted of an alteration of island with shallow water basins (western part PB) and deep marine depressions (GHP). In the peripheral areas sedimentation kept pace with subsidence and shallow water conditions existed, but in the central area of the GHP, which was far away from the sources of clastic influx, starved basins with water depth in excess of 1000 m developed (Lenkey, 1999).

As the western part of the Pannonian Basin underwent a late stage of neotectonic uplift, the GHP underwent continued subsidence. Lenkey (1999) estimated the amount of erosion due to the inversional uplift (200-300 meter) by comparting the porosity-depth trends from the western and eastern parts of the Pannonian Basin. He concluded that the porosity-depth curve of shales from the western part of the basin can be brought into almost perfect fit with the curve deriving from the GHP by a downward shift of 300 m. Similarly, for sandstones this fit is accomplished with a 700 m downward shift. At the same time several assumptions were made. The decrease in porosity is only due to burial and compaction, and uplift and erosion do not cause decompaction of the sediments, the fit of the two porosity-depth curves means that 300 m erosion occurred in the western part of the basin (Lenkey, 1999).

The methodology used to create a new porosity-depth curve for the research area is based on the former porosity-depth relationships for shales and sandstones constructed by Szalay, 1982 (Fig. 12). The porosity-depth relation is used in the decompaction process during the reconstruction. The analysis consists of four substantial steps.

First of all, the porosity-depth curves are reconstructed with the application of pre-defined equations (Fig. 12). Secondly, the shale/sand ratio data (appendix E) is combined with these porosity-depth curves (c.f. Szalay and Szentgyörgyi, 1988; Uhrin and Sztanó, 2012) in order to define the effective porosities as function of the depth for wells; Gyekenyes-1, Tarany-2, Felsoszentmarton-1 and Semjanhaza-3.
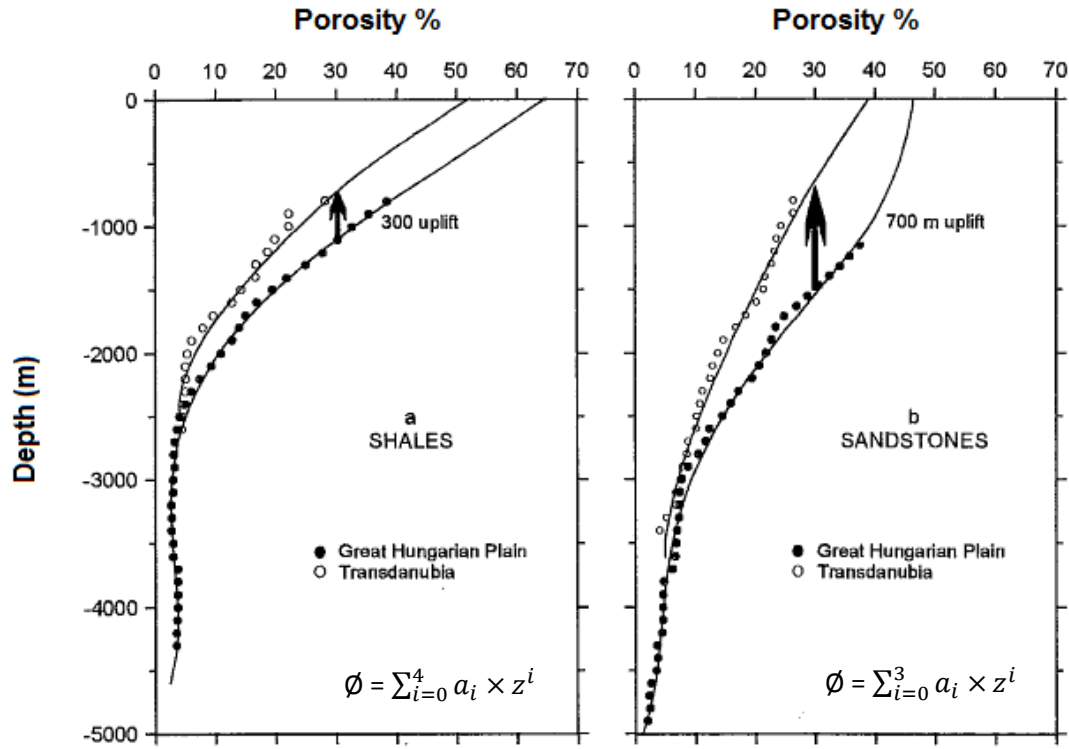
Figure 12: Porosity-depth trends (Szalay, 1982) for a) Shales and b) Sandstones. The formula for both curves is shown in the lower right corner of the graph (modified after Lenkey, 1999).

A subsequent extrapolation of the effective porosities outside the shale/sand ratio data is necessary in order to construct a full porosity-depth curve. The extrapolation is necessary mainly for the shallower part of the curves and correlated by 4 different wells.

Finally, an average of the different wells is taken in order to construct a new generalized porosity-depth curve for the defined cross-section.

The cross-section reconstruction

Midland Valley's MOVE 2015 software was used as a tool for reconstructing the defined cross-section in the research area. The same as for Petrel, the Hungarian EOV coordinate system is set as default (appendix C).

The actual workflow for the restoration consists of several different steps (Fig. 13). The first part is the model building, in which the cross-section is constructed and the subsequent stratigraphic model is set. A simple time-depth conversion is then performed on the cross-section. This is followed by setting the decompaction function parameters with the newly determined porosity-depth relation. Finally, a 3 step loop workflow is used to restorate the palaeobathymetry. Elaboration on the different steps is given in the next paragraphs.
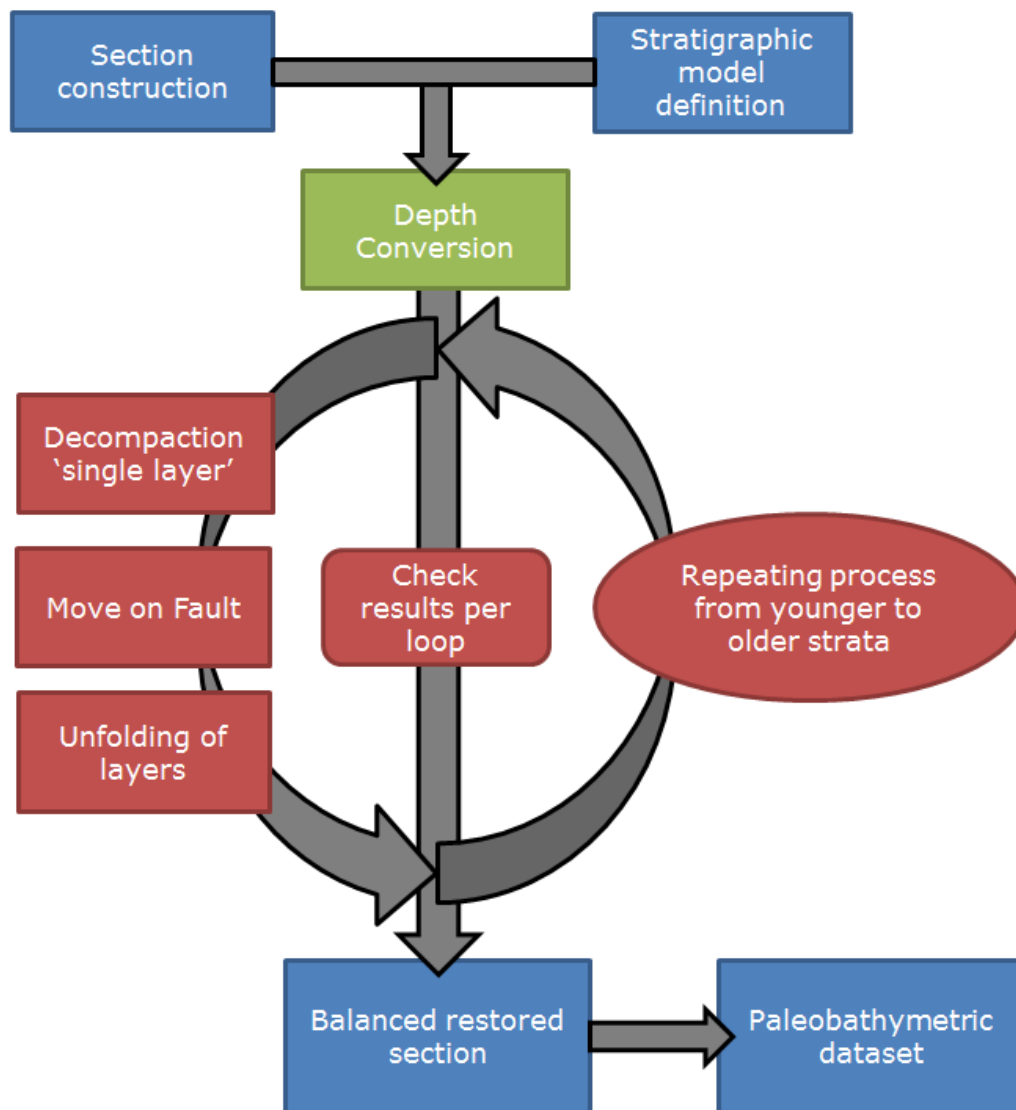
Figure 13: Workflow section restoration in MOVE.

Time-Depth conversion

A process of time-depth conversion was applied to the constructed cross-section. The V_0-K method (Smallwood, 2002) used follows the function:

$$V_{inst} = V_0 + Kz$$

V_{inst} = Instantaneous velocity.

V_0 = reference velocity or initial velocity (m/s).

K = velocity gradient.

z = depth (m).

Figure 14: Schematic figure showing the difference in interval velocities between horizons (Midland Valley - MOVE, 2015).
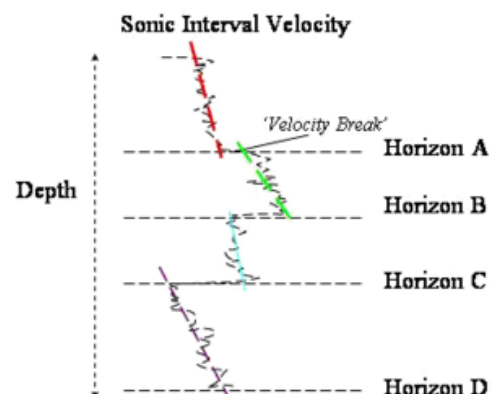
An average time-depth curve was estimated by plotting all checkshot data in one single function diagram. The V_0 and K were then estimated as linear relationship (Fig. 14) of the interval velocities (m/s) as function of the depth (m).

In the MOVE software the time depth conversion follows then the following linear function:

$$z = \left(\frac{V_0}{K}\right) x \left[(e^{Kt}) - 1\right]$$

z	= resultant depth (m).
e	= natural logarithmic base.
t	= one way travel time (s).

Decompaction

Compaction of sediment layers is assumed to be the irreversible process in which a reduction of pore space and rock volume is realized as a consequence of pressure increase due to burial by younger stratigraphic layers. Loss of pore space is of concern in several aspects of study of sediments and sedimentary rocks. It applies to the nature of petroleum reservoirs, to the reconstruction of original sedimentary structures, and to the reconstruction of patterns of subsidence in a sedimentary basin (Baldwin and Butler, 1985).

There are two different types of compaction (Fig. 15): 1) equilibrium (normal) compaction, and 2) disequilibrium compaction. During equilibrium compaction, the porosity and permeability decreases with depth following a linear decrease. Disequilibrium compaction occurs in sedimentary basins during rapid burial, when the pores are getting isolated at depth and the retained fluid overpressured (Osborne and Swarbrick, 1997; p. 1023-1041). In the SW Pannonian Basin the zone that exhibited disequilibrium compaction is found between 2500 and 3000 m (Horvath et al., 2015).

The process of decompaction allows the reverse modelling of the effects of rock volume change due to porosity loss with burial. The zone of interest for the decompaction process is the prograding shelf-margin, with a special interest for the Algyö Fm. (Fig.11). This formation is buried in the research area between a few hundreds of meters up to 2 kilometers in depth. This means that the formation was buried under the influence of normal compaction. Moreover, as the late Miocene to Quaternary is an interval with mixed lithologies, according to well data (appendix E); the recommended method for the decompaction process follows the function set by Sclater and Christie (1980). As a consequence the use of the Athy relationship is justified for the process in MOVE:

Athy's relationship;

$$f = f_0(e^{-cy}) \qquad (Athy, \ 1930; \ Rubey \ and \ Hubbert, 1959)$$

f = present-day porosity at depth

f_0 = initial porosity at surface conditions

c = Porosity-depth coefficient: rate of change of porosity with depth
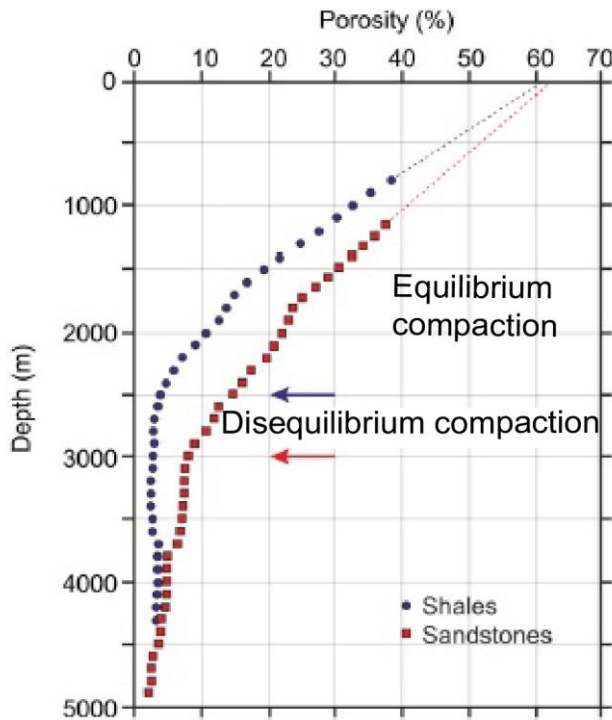
y = depth (m)

Figure 15: Results of porosity determinations as function of depth for both shales and sandstones in the Pannonian Basin. Disequilibrium compaction from about 2500-3000 m leads to isolation of pores and fluid retention (modified after Spencer et al., 1994 and Horvath et al., 2015).

3 step loop process

The process of reconstructing the development of the prograding shelf slope margin consists of a number of steps (Fig.16). Essentially, the restoration consists of a 3 step loop process. All tectonic processes, including subsidence and deformation to the stratigraphic section, are sequentially removed. This restoration follows a reversed order from younger to older. An essential part of the restoration is checking each performed step on geological validity. (1) First step of the loop is removing a 'single' sediment layer followed by the associated isostatic ('airy') unload and decompaction of the remaining layers. In areas where basement deformation is absent or minor, variations in the net load have long wavelengths, occurring over broad areas rather than locally, and 'airy' (one-dimensional) isostasy is an acceptable simplification of the more realistic flexural response of the crust (Roberts, 1995; Midland Valley - MOVE, 2015). Simultaneously, the amount of decompaction is determined, as discussed in the previous paragraph. (2) The next step is the restoration of the fault movement during the different episodes of inversion in the region. An estimation of amount per step of the restoration is determined by the use of indicator horizons next to and above the fault plane.

(3) Finally, large-scale folding and thermal subsidence needs to be reversed by the use of the process of unfolding. The total process is repeated until the horizon of interest (shelf-margin) is reached and the final result, the palaeobathymetry can be determined. Uncertainties in the restorations were assessed by varying the parameters for isostatic unloading and decompaction. As Steckler et al, (1999) stated: "compaction errors arise from uncertainties in the absolute lithologies and the corresponding compaction coefficients". The amount of errors, scale with the thicknesses of the removed sediments. Thus, the largest errors occur at the thicker part of the sediment sequence.
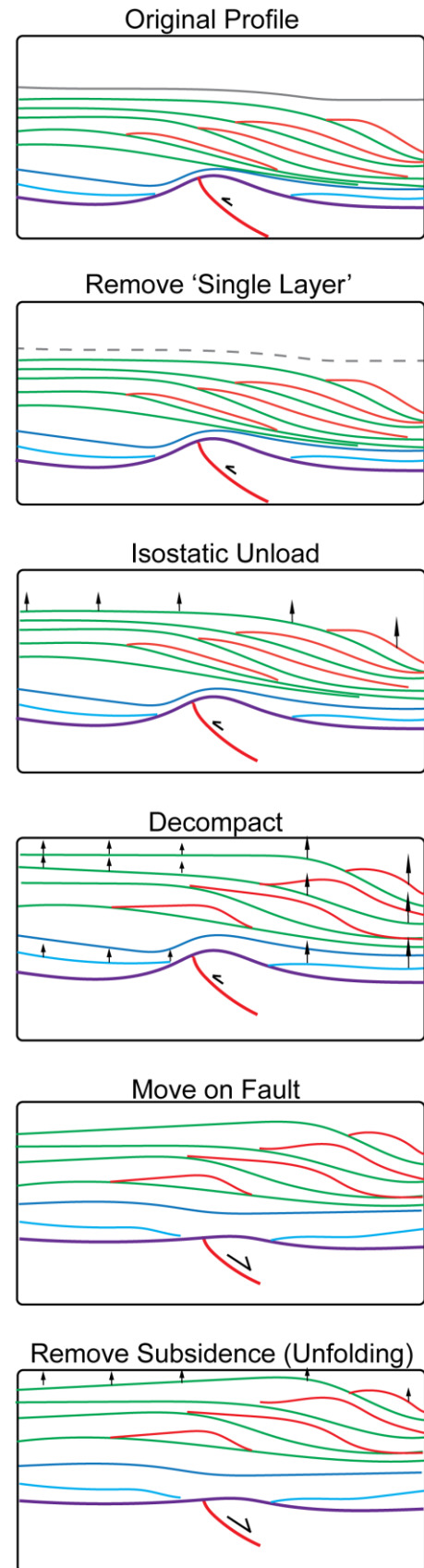
Original Profile

Remove 'Single Layer'

Isostatic Unload

Decompact

Move on Fault

Remove Subsidence (Unfolding)

Figure 16: Schematic figure showing restoration steps (modified after Lavier et al, 2000).

Results

In this paragraph the results are given for the different steps in the previous discussed methodology. An analysis of the progradational sequence is followed by a tectono-sedimentary description of the defined cross-section (location, see Fig. 10C). Moreover, the parameters for both the time depth conversion and the decompaction process are given. Finally, the results for the cross-section reconstruction with associated palaeobathymetric dataset are visualized and elaborated via different time-shots.

Analysis of the progradational sequence

Within the progradational infill of the Pannonian Basin four seismic facies are distinguished (Fig. 17). Moreover, the Middle-Miocene graben infill can be interpreted as distinctive seismic facies, which allows for recognition between syn-kinematic to early post-kinematic transition.

The first seismic facies indicated with A, corresponds to the Middle Miocene (half-) graben infill. It is characterized by low amplitude sub-parallel or divergent discontinuous reflections. The next seismic facies (B) drapes the underlying units (A) and consists of largely (sub-) parallel, sub-flat continuous reflectors. Difference in thickness of the deposits belonging to this seismic facies is common and larger above (half-) grabens. Upslope a new seismic facies (C) is characterized by higher slope gradients. The facies has medium to low amplitude (hummocky) discontinuous reflectors. This seismic facies is representative of the turbiditic bodies of the Szolnok formation. Overlying the turbiditic bodies, the prograding foresets of the Algyö formation are indicated by (D). The foresets are characterized by an alternation of continuous and discontinuous, medium to low amplitude reflectors. Transition to the upper seismic facies is interrupted by the shelf break seen as a local drop in reflector amplitude and frequency. The seismic facies (E), occurring upslope to the shelf break, is characterized by sub-parallel fairly continuous, high amplitude reflectors and representative for the Újfalu Fm.

A clear representative example (Fig. 18) of the prograding system during Pannonian times shows the lateral positioning of the different seismic facies (Fig. 17).
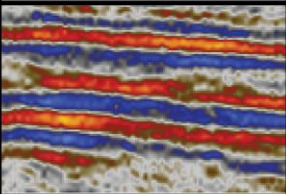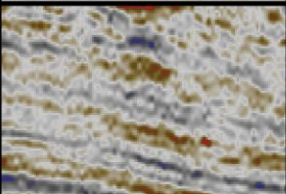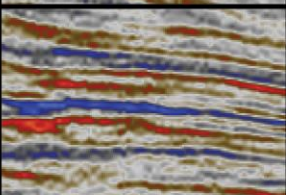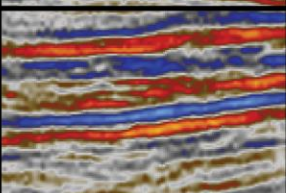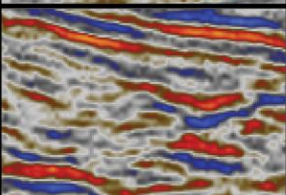
Seismic Facies	Seismic example	Characteristics	Amplitude and frequenctie	Formation and depositional environment
E		Sub-parallel fairly continuous	High amplitude, high frequency	Fluvial and delta deposits of the Újfalu Fm.
D		Clinoform Alternation of continuous and discontinuous	Medium to low amplitude, high frequency	Shelf slope deposits of the Algyö Fm.
C		Hummocky discontinuous or sub-parallel fairly continuous	Medium to low amplitude, high frequency	Turbiditic bodies of the Szolnok Fm.
B		(Sub-)parallel sub-flat continuous	Medium to high amplitude, low to high frequency	Deep hemi-pelagic deposits of the Endröd Fm.
A		Sub-parallel continuous to non-continuous	Low amplitude, medium to high frequency	Shallow marine Middle Miocene deposits

Figure 17: Seismic facies used in the seismic interpretation of the prograding shelf-margin (fig. 11) and the transition between pre-Pannonian and Pannonian. Terminology follows the seismic interpretation and seismic stratigraphy of clastic depositional facies by Sangree and Widmier, (1978).

A representation of the alternation of progradation (red), and retrogradation (green) is visualized (Fig. 18, green and red clinoforms). The different progradational clinothems are separated by retrogradational clinothems. Clear reflection terminations are interpreted in the progradational bodies (toplaps or onlaps on retrogradational clinoforms). This leads to the exclusion of a regional unconformity separating the Algyö shelf-slope sediments and the Újfalu shelf sediments.

Overlying the prograding sequence a clear unconformity marks the Miocene-Pliocene boundary. This unconformity is characterized by onlapping and slighty rotated reflectors corresponding to the Zagyva Formation. This boundary also marks the transition from shallow delta and fluvial to a terrestrial and alluvial deposition environment.
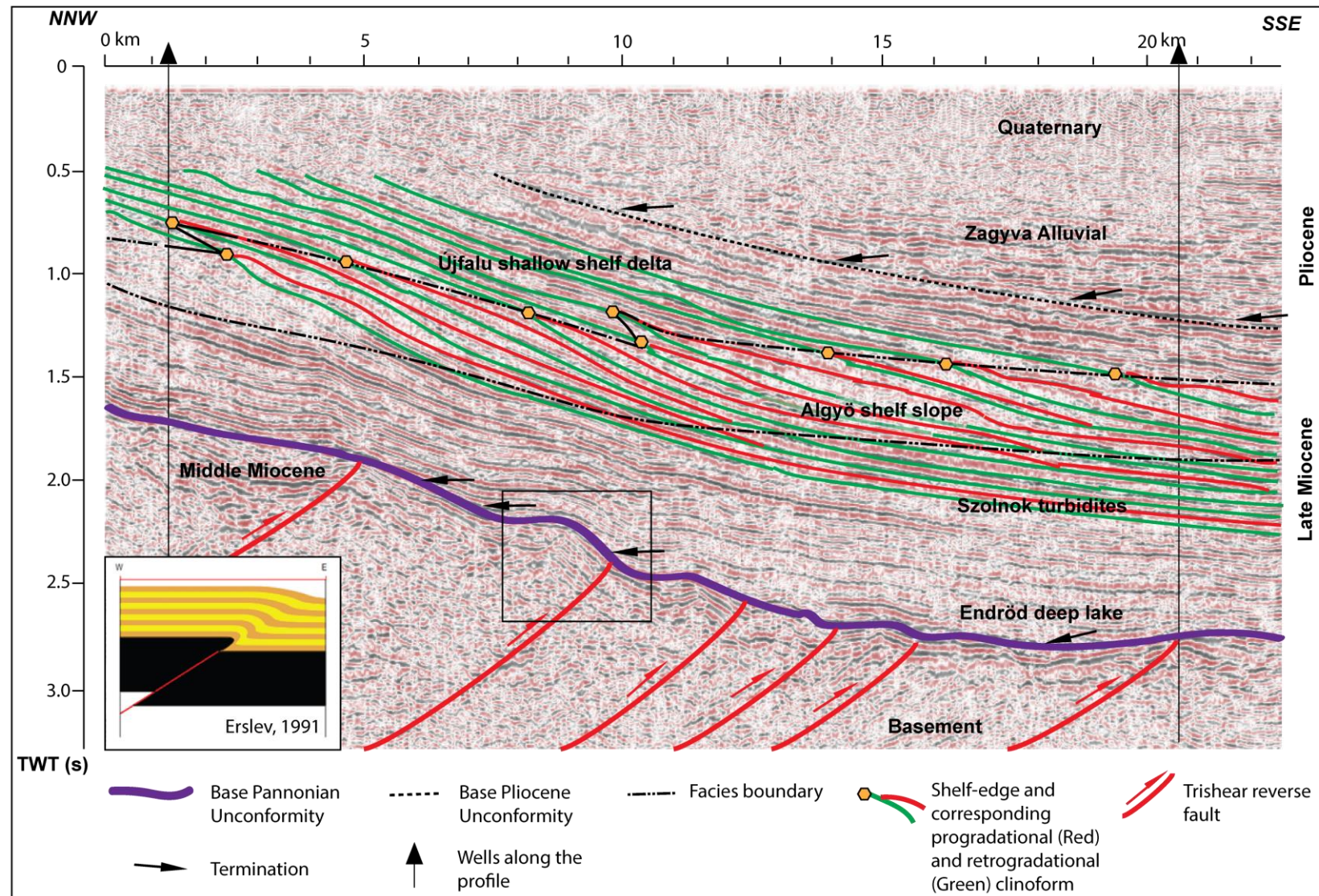
Figure 18: Seismic section (D4_migr) from the Drava Through showing the typical basin fill succession in SW Hungary. This section clearly shows that the progradational body consists of an alternation of progradation (red), where deposition started at the shelf-margin, and retrogradation (green), where deposition also occurred on the shelf. This alternation of clinothem bodies rules a regional unconformity out. For location, see figure 10. In the left bottom corner a schematic figure of a trishear reverse fault is shown (Erslev, 1991). This figure illustrates the fault and folding kinematics representative for all the faults interpreted in this figure. The black square indicates the exact position of this trishear kinematic behavior.

Tectono-sedimentary description of the defined cross-section

Using these results of the cross-section (location, see Fig. 10C) a balanced tectono-sedimentary history can be made. The entire cross-section is divided into two different sections (Figs. 19 A&B). A clear alternation of paleo-highs and depocenters is present in the entire cross-section.

Middle Miocene structural observations

The pre-Neogene extension, corresponding normal faulting, and the initiation of the Pannonian Basin formation is supported by several observations throughout the section. Starting at the Inke High (Fig. 19A, ~20-25 Km), the Middle Miocene (light blue) is characterized as an asymmetric depocenter formed along two, SE and NW dipping, normal faults. Both faults show a large normal offset. However, an asymmetric depocenter geometry is present, as the NW dipping fault clearly has a higher offset than the SE dipping fault. Moreover, a layer thickening is observable in both the north and the south towards the boundary faults.

More to the south of the section (Fig. 19B) both the Nagykanizsa and the Tarany subbasins show thinning of the middle Miocene sequence towards the north and south flanks. For the Nagykanizsa subbasin the thinning towards the north is partly outside the defined section (see Fig. 6). In the Tarany subbasin two SE dipping small offset normal faults are present. The same applies for the normal fault at the southern margin of the Nagykanizsa subbasin. Furthermore, a difference in thickness of the middle Miocene sequence is notable between grabens (Inke High) and half grabens like the Tarany subbasin.

Lastly, a combination of chaotic low amplitude reflectors just above strong amplitude reflectors is noticeable in the deepest part of the depocenter under the Inke high, suggesting the rifting in this area to be late Early Miocene to early Middle Miocene.

Middle-Late Miocene boundary and associated inversion

The Middle Miocene rifting is followed by an episode of compression and inversion at the start of the Late Miocene. This transition is marked by a strong diachronous erosional unconformity (purple line, Figs 19A&B). However, depending on the paleographic position in the Pannonian Basin, namely in the basin centers, the base Pannonian can be interpreted as a correlative conformity (Fig. 11). Interpretation of this unconformity is supported by termination of the high amplitude reflectors on top. Both onlaps (at basinal margins) and downlaps (at basinal centers) mark this unconformity.

Figure 19A: Interpreted composite reflection seismic transects from the SW part of the Pannonian Basin. The section shows the main tectonic and stratigraphic features in the area. This section represents the northern part of the total defined cross-section in this study. The southern part is shown in figure 19B. For location of the cross-section see figure 10. Ages of the prograding shelf edges are derived from Magyar et al., 2013, see Fig. 3.

Early Late Miocene paleo-relief was characterized by an alternation of depressions and highs. The episode of compression at the beginning of the Late Miocene caused the inversion and reverse cross-cutting of Middle Miocene normal faults, causing the formation of positive pop-up structures as can be seen below the Inke High (Fig. 19A) and the northern margin of the Tarany subbasin (Fig.19B). Furthermore, at the margins of the subbasins, low-offset high-angle reverse faults inverted earlier normal faults and are associated with small anticlines in the Middle and early Late Miocene sediments.
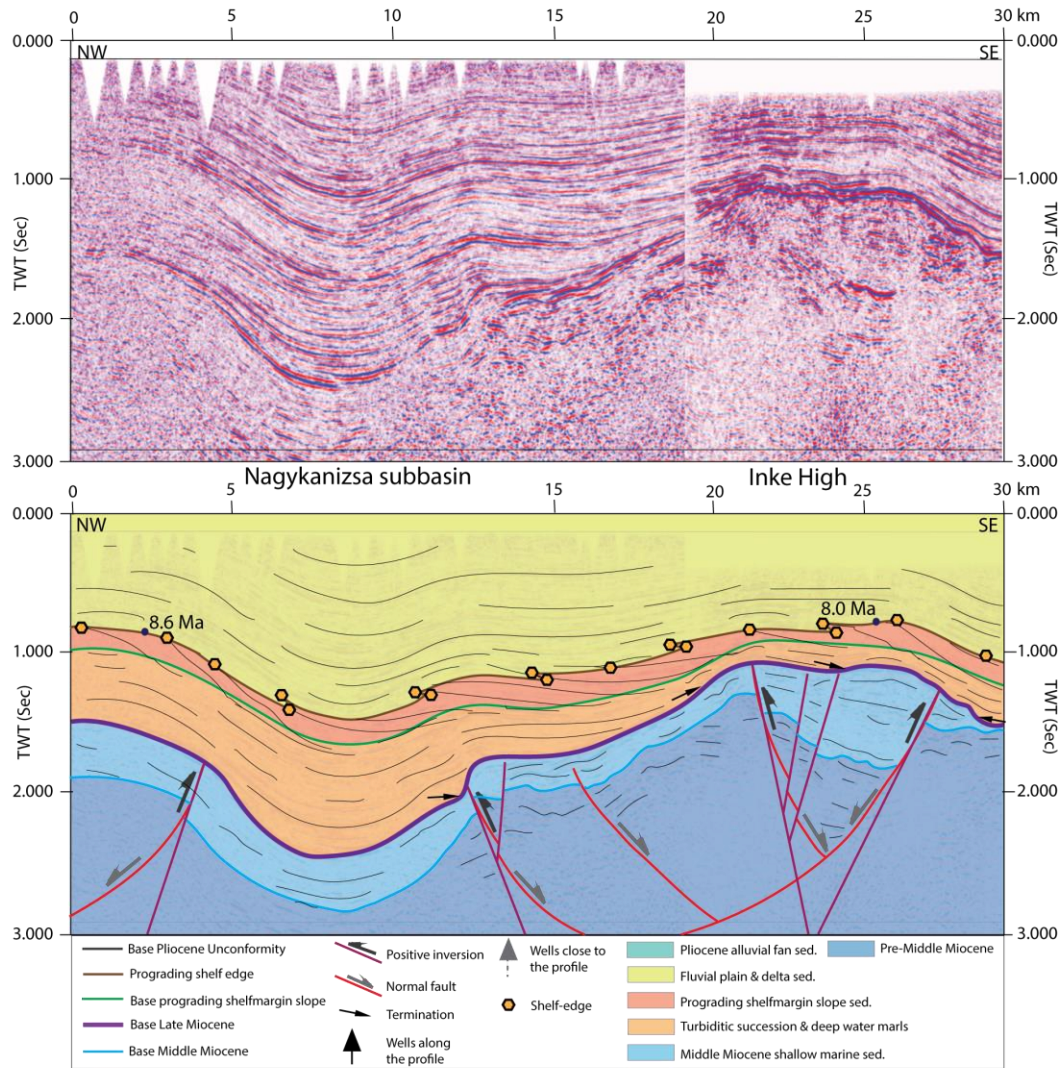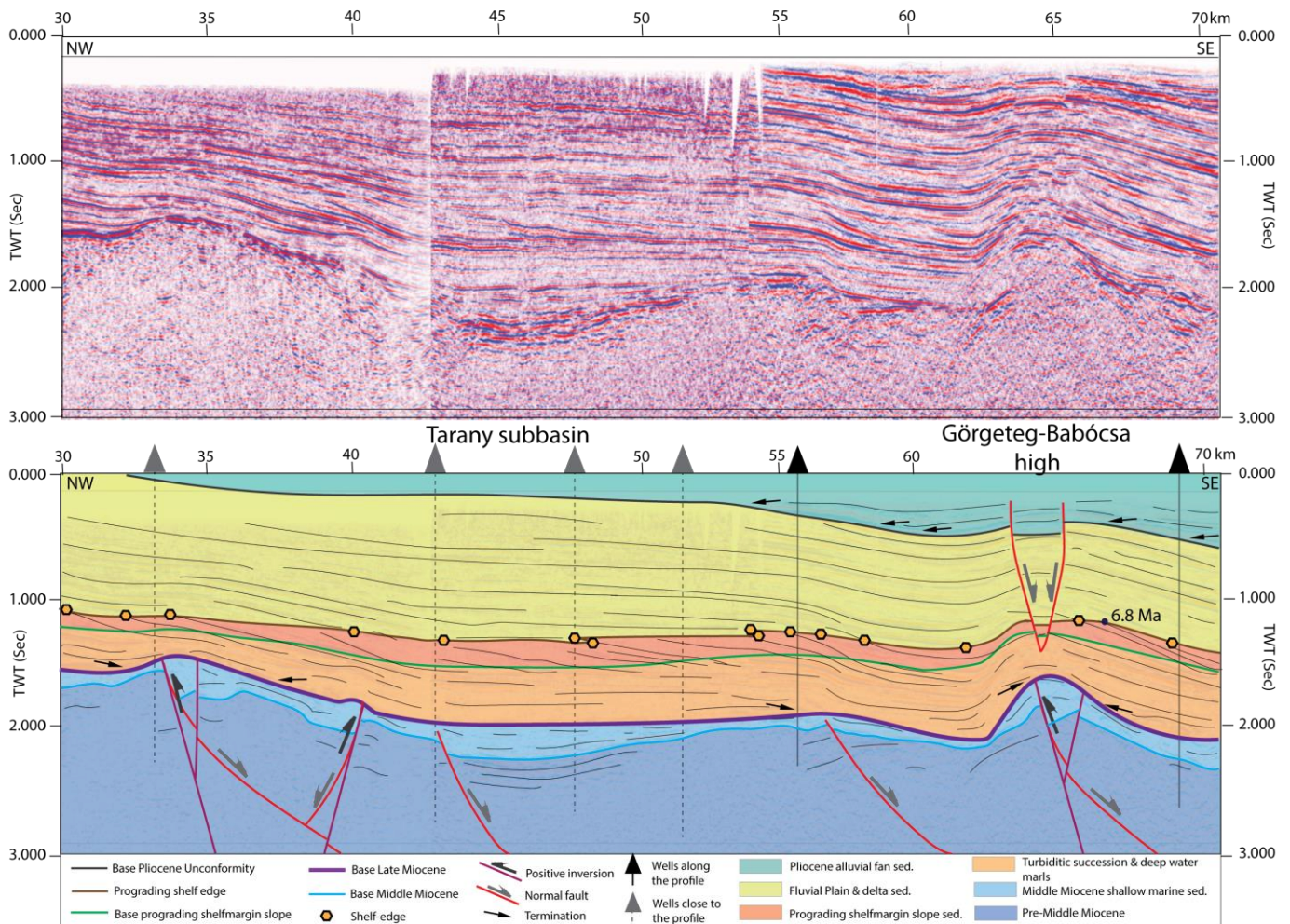
Figure 19B: Interpreted composite reflection seismic transects from the SW part of the Pannonian Basin. The section shows the main tectonic and stratigraphic features in the area. This section represents the southern part of the total defined cross-section in this study. The northern part is shown in figure 19A. For location of the cross-section see figure 10. Ages of the prograding shelf edges are derived from Magyar et al., 2013, see fig. 3.

Late Miocene progradation and subsidence

The diachronous termination of this period of compression and inversion was followed by rapid thermal subsidence in the basin centers. During the early Late Miocene the existing paleo-relief was subsequently filled by deep hemi-pelagic sediments, onlapping at basin margins and downlapping in the depocentres and at existing basement highs. A strong difference in thickness of these sediments is well visible between the Nagykanizsa subbasin and above the Inke High.

This period was followed by the initiation of the prograding sequence starting in the NW moving on to the SE. Already existing Middle Miocene (half-) grabens were either filled or overfilled by this diachronous system.

Moreover, during this period the rate of subsidence increased further as the thickness of the prograding sequence required large palaeobathymetries. This is also seen in the large thickness difference of syn-kinematic Middle Miocene (~1.5 km) and overlying Pannonian sediments (~3.5 km).

Late Miocene-Pliocene boundary

The transition, between the delta and fluvial sediments of the Late Miocene, and the alluvial and terrestrial sediments of the Early Pliocene, is marked by an erosional unconformity at basin margins and a conformable conformity at basin depocenters (dark grey horizon, fig. 19B). This unconformity is characterized by onlap of Pliocene sediments, which are slightly rotated to sub-horizontal. For this cross-section, from the depocenter no real evidence is found for large-scale incision at the base Pliocene.

Pliocene to Quaternary inversion

The visible rotation of reflectors above the base Pliocene unconformity, together with the high amplitude asymmetric folding of the Pannonian sediments indicates a late stage of major basin inversion. This inversion led to the reactivation of Middle Miocene cross-cutted faults. Moreover, normal faults, with increasing offset towards the top, (Fig. 19B, ~65 km) and the syn-sedimentary deformation resulting in the Pliocene to Quaternary sedimentary wedge support an ongoing late stage inversion.

Time depth conversion and Porosity-Depth curve

The parameters obtained from the checkshot analysis are used in the time-depth conversion process. In the graph (Fig. 20) the depth (m) is given as function of the interval velocity (m/s). Deriving a linear relationship *(V_{inst} = 1938 – (0.78 x Z))* following the commonly used V_0-K method leads to an equation representative for the research area, resulting in an incorporated initial velocity (V_0) of 1938 m/s and a velocity gradient (K) of -0.78.
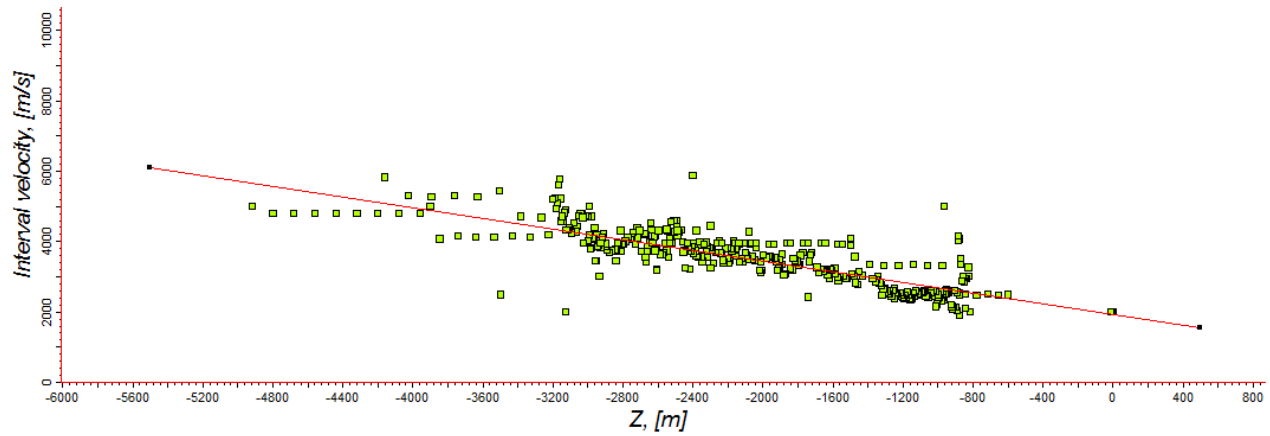
Figure 20: Graph showing the depth (m) as function of interval velocity (m/s). The green dots represent the checkshot data available in the area. The red line shows the linear relationship ($V_{inst} = 1938 – (0.78 \times Z)$) of the V_0-K method (Smallwood, 2002

Subsequently, the porosity analysis provides us with a representative porosity-depth (Fig, 21) curve for the Neogene sediments.

$$f = 52.6 \times e^{(-5.8*10^{-4} \times y)}$$
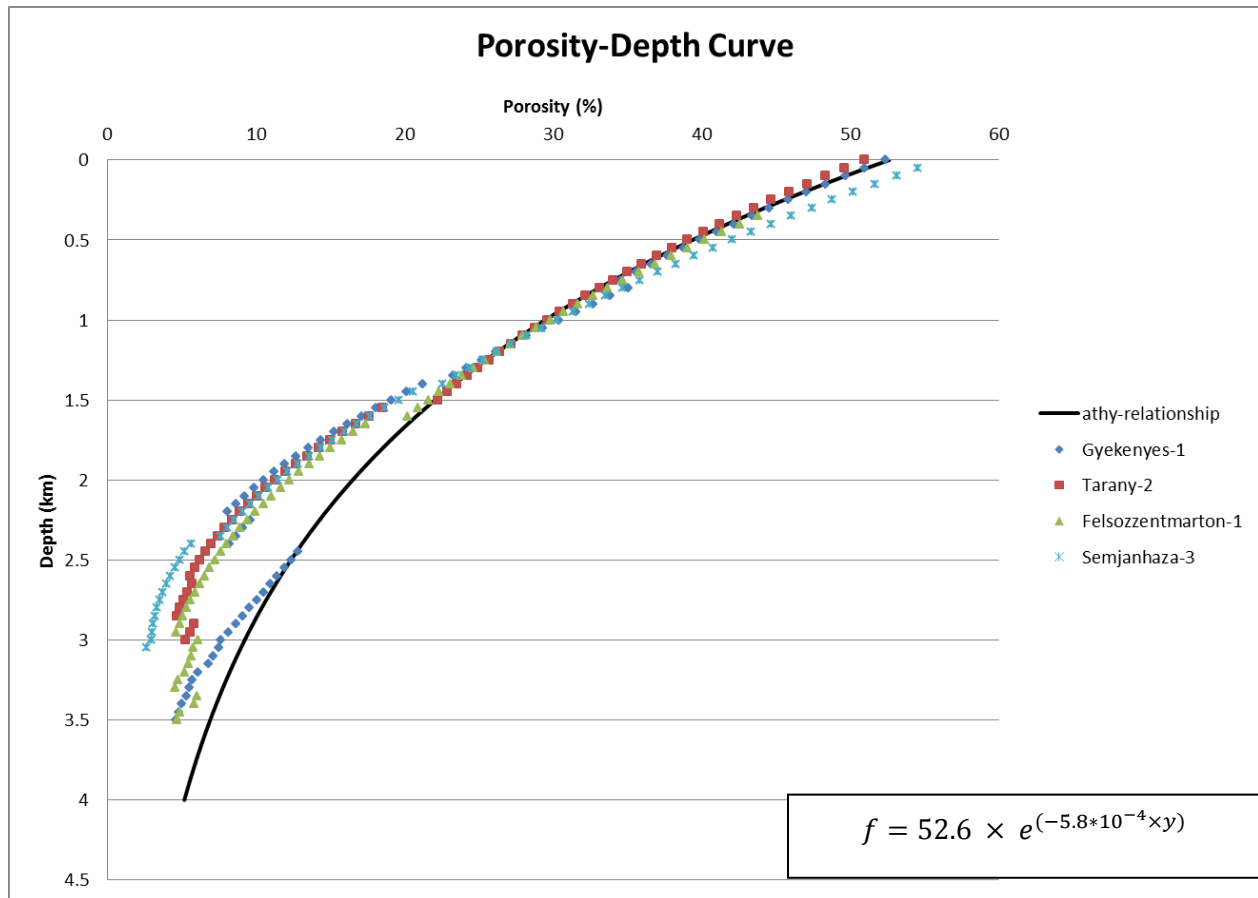
Figure 21: Porosity-depth curve representative for the Neogene sediments up to 1.5 km. The corresponding relationship is shown above the legend. This porosity depth curve is modified after Szalay, 1982 and Lenkey, 1999; using shale/sand ratios from well data (Gyenkenyes-1, Tarany-2, Felsozzentmarton-1 and Semjanhaza-3) in the area.

Note that the black curve significantly deviates from the data points below 1.5 km depth. Starting at the deepest points a drop of porosity occurs between 2.5 - 3 km depth. This drop is related to the transition of Middle Miocene to Late Miocene sediments. At the end of the Middle Miocene shallow marine sediments dominated. Whilst at the beginning of the Late Miocene, the deep hemi-pelagic marls of the Endröd formation occurred. A second transition in porosity is noticeable at ~1.5 km, where a sudden increase in porosity occurs. This porosity increase is related to the transition from fluvial and delta sediments (latest Late Miocene) to more terrestrial alluvial sediments (Early Pliocene).

The black curve corresponds to the best-fit relationship for the decompaction process of Neogene sediments. The associated initial porosity (f_0) is 52.6% and the depth coefficient (c) is 0.58 per km.

Palaeobathymetric reconstruction

In this paragraph the results of the different sequential steps (Fig. 22) of the cross-section reconstruction are given.

The first step (Fig. 22a) corresponds to the entire section (Fig.19A&B) in time domain. In this section 7 episodes of retrogradation or aggradation are identified (see also, Fig. 19A&B).

Next, the V0-K method is used to convert the section in depth (Fig. 22b). Moreover, the normal faults, present in the time section (Fig. 22a), above the Görgeteg-Babócsa high, are reconstructed with increasing offset (~25-80m) towards the top. Furthermore, 14 palaeobathymetric data points are identified with vertical dotted lines.

From the depth section (Fig. 22b), the next step is decompaction of the Pliocene to Quaternary sediments, resulting in the Base Pliocene unconformity to be situated approximately ~100-200 m below the surface (Fig. 22C). Moreover, the neotectonic folding, above the Görgeteg-Babócsa high, is partly flattened by vertical movement along the fault. This results in a vertical movement of ~50 m and a horizontal extension of ~30 m.

After decompaction of the upper most strata (Fig. 22c), the unfolding of the base Pliocene unconformity towards the surface is performed, simultaneously restoring basement subsidence (Fig. 22d). The amount of uplift varies from 100 m in the Northern to a maximum of 300 m in the Southern part. Furthermore, the unfolding restores the slight tilting during the Pliocene to Quaternary deposition.

Unfolding of the base Pliocene unconformity at the surface (Fig. 22d) is followed by the removal and decompaction of the shelf sediments (Fig. 22e). Furthermore, fault movement along all major faults in the section partly flattens the neotectonic folding of the shelf-edge trajectory. This results in a vertical movement ranging between ~20-60 m and a horizontal extension of ~110 m.

Lastly the shelf-edge trajectory (Fig. 22e) is unfolded and decompacted, resulting in increased foreset heights (Fig. 22f). The unfolding further restores basement subsidence and the uplift is ~500 m. This results in a total differential basement subsidence for this section ranging between 600 m and 800 m.

The resulting palaeobathymetric dataset (Fig. 22f) includes the 7 phases of retrogradation, increasing the water depth by max ~80-100 m. Moreover, the same 14 data points (Fig. 22b) are visualized with the vertical dotted lines.

The most interesting part of these results is the comparison between the depth section (Fig. 22b) and the foreset decompacted section (Fig. 22f). The increase in height of the foresets is clearly noticeable and measured along the 14 data points. For the depth section (Fig. 22b) the height is measured perpendicular to the dip of the deformation. On the other hand, the height of the decompacted foresets (Fig. 22f) is measured vertically.

The difference in height and the ratio of increase varies (Fig. 23) between the paleo-highs and depocenters. For data point 3, representing the deepest part of the Nagykanizsa subbasin, the ratio of increase is 1.8. At the same time, the ratio of increase on the Inke high (point 4 and 5) is only 1.4 or 1.5. Point 9 in the Tarany subbasin has a ratio of 1.6. The other 10 data points indicate a ratio of increase of 1.5.

A palaeography division (Fig. 23) is made into highs, lows and the direct intermediate areas. The overall height of the foresets (Fig. 23) reaches a maximum of ~420 m in the Nagykanisza subbasin and a minimum of ~150 m on the Inke high. Moreover, the height in the intermediate areas is relatively high compared to the paleo-highs.
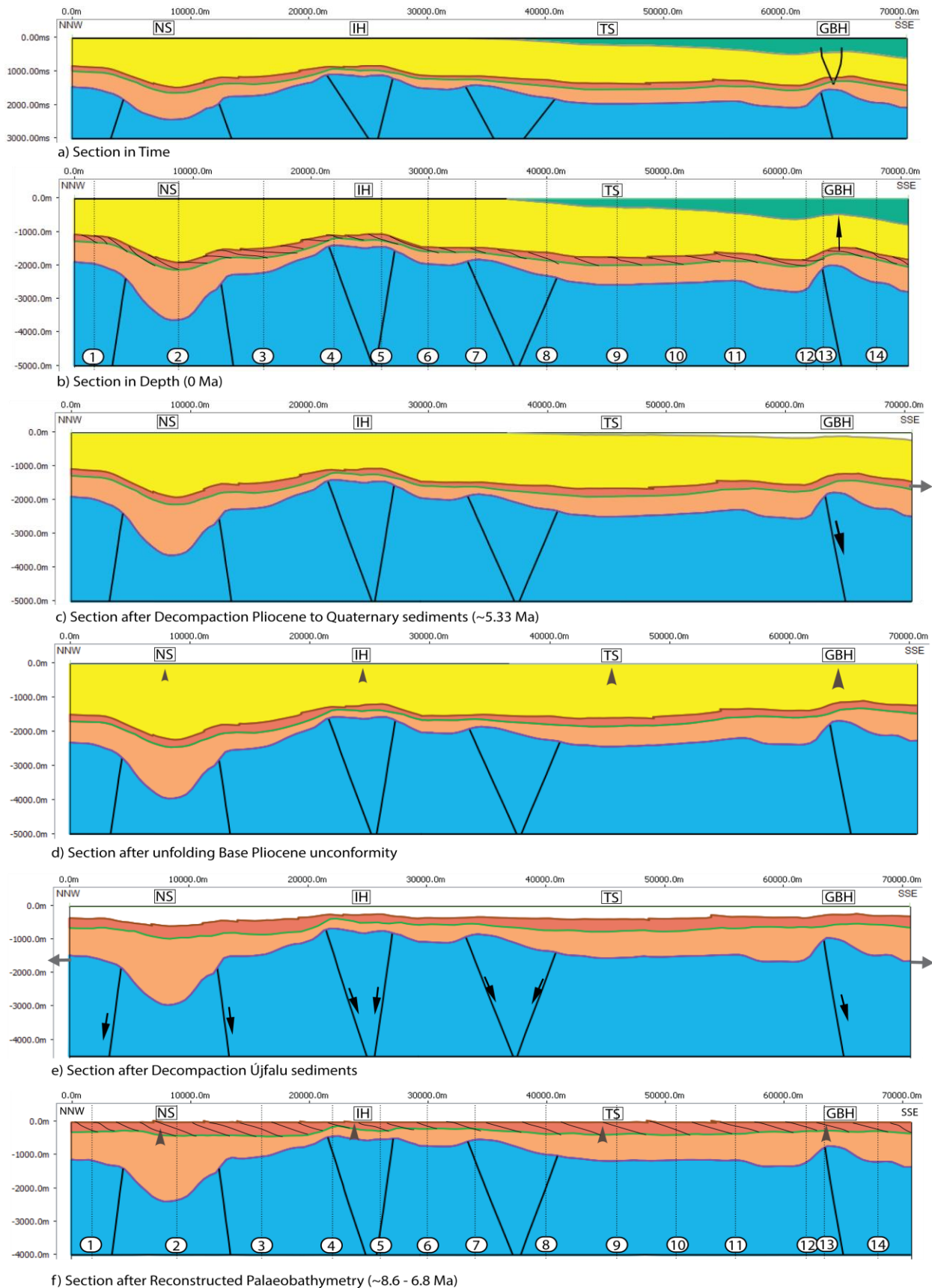
Figure 22: Sequential reconstruction (using MOVE) of depth-converted interpreted seismic section from SW Hungary. a) Time section; b) Depth section with reconstructed compaction fault ; c) Decompaction Pliocene to Quaternary sed.; d) Unfolding base Pliocene unc.; e) Decompaction Újfalu (shelf) sed.; f) Final section with reconstructed palaeobathymetry. Abbreviations; NS: Nagykanizsa subbasin; IH: Inke high; TS: Tarany subbasin; GBH: Görgeteg-Babócsa high. Stratigraphic unit; Green: Pliocene to Quaternary sed.; Yellow: Újfalu (shelf) sed.; Red: Algyö sed.; Orange: Szolnok and Endröd sed.; Blue: Pre-Pannonian.

40

Point	Position along section (m)	Height foreset (Fig.22b) in m	Decompacted height (Fig.22f) in m	Ratio
1	1700	192	289	1.5
2	8800	210	385	1.8
3	16000	284	416	1.5
4	22000	97	146	1.5
5	26000	185	264	1.4
6	30000	130	198	1.5
7	34000	130	195	1.5
8	40000	239	355	1.5
9	46000	230	363	1.6
10	51000	247	380	1.5
11	56000	225	346	1.5
12	62000	177	265	1.5
13	63500	176	263	1.5
14	68000	173	265	1.5
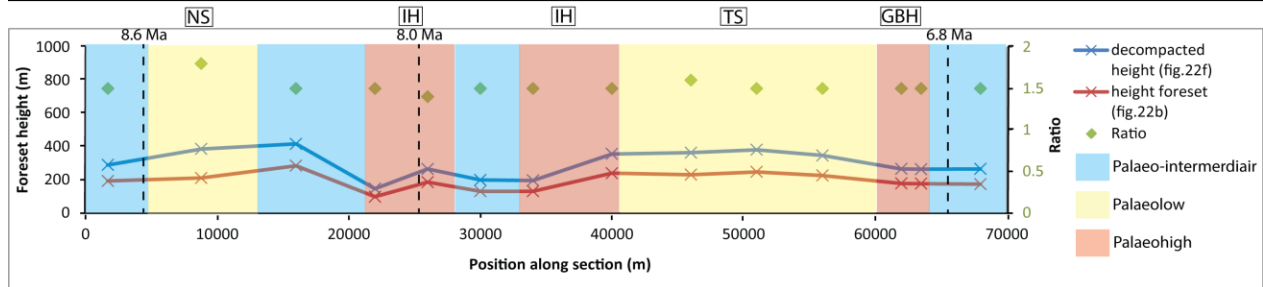
Figure 23: Chart and graph showing the palaeobathymetric evolution of the section (Fig. 22) in SW Hungary. 14 palaeobathymetric data points are listed (for location, see Fig. 22b and 22f). The ratio indicates the multiplication of increase of the foreset heights after the process of decompaction. The graph visualizes the information in the chart above. Ages (8.6 – 6.8 Ma) of the prograding shelf edges are derived from Magyar et al., 2013, see fig. 3. Abbreviations; NS: Nagykanizsa subbasin; IH: Inke high; TS: Tarany subbasin; GBH: Görgeteg-Babócsa high.

Discussion

My study demonstrates that there is a difference in palaeobathymetry level during the Late Miocene phase of progradational infilling of the SW Pannonian Basin. The results show that the prograding foreset heights varied ca. 150-420 meters along the interpreted section in a time span of ~2 Ma. In this chapter further emphasis will be given on the different forcing factors resulting in these fluctuations. Moreover, the regional evolutionary model is discussed and linked to the palaeobathymetric results. Lastly, a short review is given on the applicability of these results in future research.

Paleo-water depth evolution and its forcing factors

My palaeobathymetric reconstruction showed that over a timespan of nearly 2 million years (8.6-6.8 Ma, shelf-edge ages taken from Magyar et al., 2013) several fluctuations in decompacted foreset heights are found. The thickness difference reaches up to ~270 m (Fig. 23). Moreover, a variation in the ratio of increase between foreset height and decompacted height is presented. In depocenters such as the Nagykanizsa subbasin this ratio can reach up to 1.8 and can be as low as 1.4 above the basement highs, as for instance, the Inke high. We can further analyse several different forcing factors (Fig. 24A), which influence the overall height of the prograding clinoform and the associated paleo-water depth.

In order to address these forcing factors, it is necessary to link the water level of Lake Pannon to a base level (Fig. 24B). This means that the base level is set as the initial accommodation space at the start of the progradation, resembling the relative sea level. However, in contrast to marine environments, in a lacustrine setting the base level can stay constant when the volume water mass stays constant. This is however only the case if all forcing factors influence the basin homogeneously. This is obviously not the case in a diachronous and asymmetric system as the Pannonian Basin.

All forcing factors sum up the resulting accommodation space, possibly leading to a large difference during sediment deposition. The main forcing factors that will be discussed here are: climate, syn-sedimentary tectonics (uplift and subsidence), differential compaction and the initial accommodation space (paleo-relief) available before the onset of progradation (Middle and Late Miocene boundary).
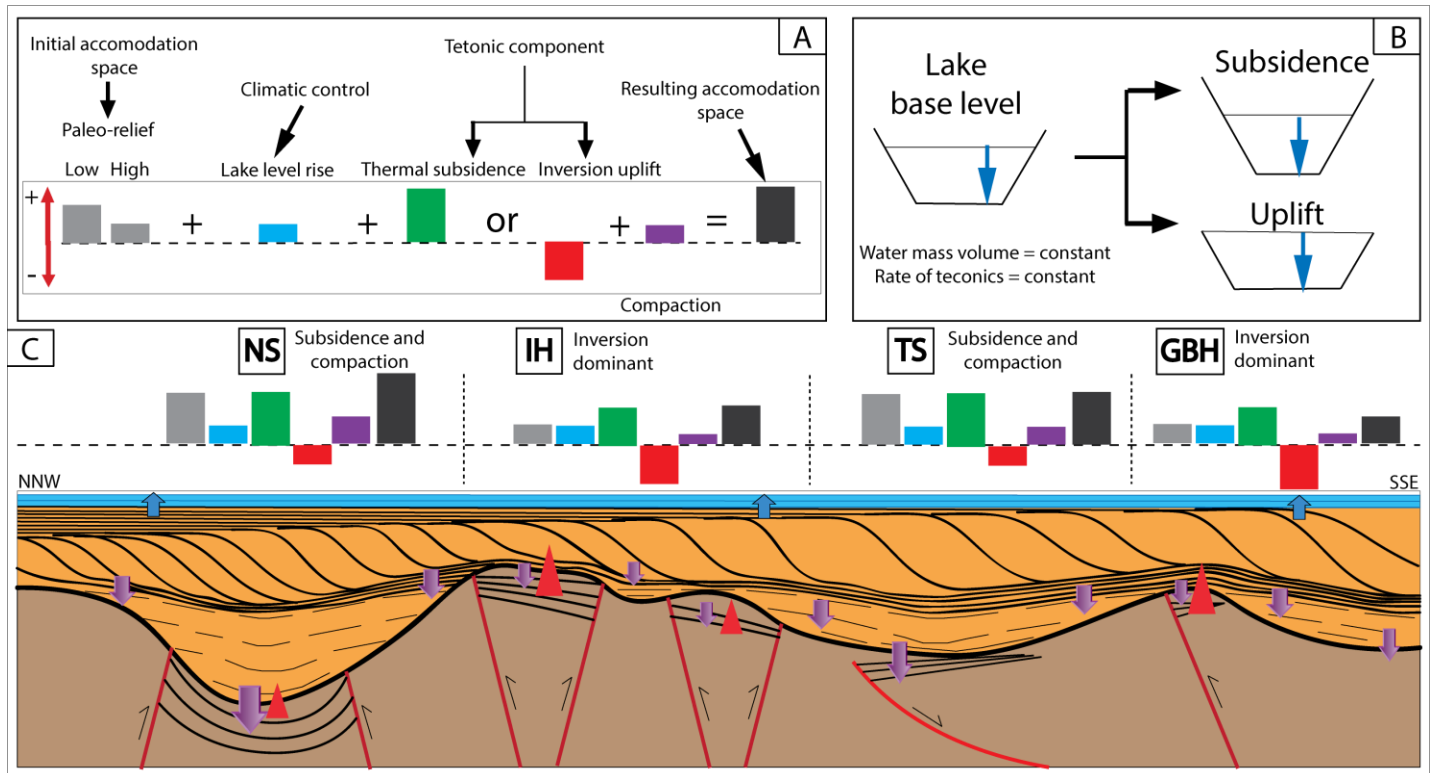
Figure 24: Illustration of the effects of forcing factors on the infill of the Pannonian Basin (cf., ter Borgh et al., 2015). The forcing factors vary in space and time. A) The resulting accommodation space available at a certain location is dependent on the combined effects of the different forcing factors. B) The lake base level does not directly change due to tectonics such as subsidence and uplift. This is only the case if water mass volume and the rate of tectonics is the same. When water volume or rate of tectonics varies the base level can rise of fall. C) Schematic figure of the cross-section in SW Hungary, showing the relative amplitudes of forcing factors. The different forcing factors are indicated with colored arrows; Blue: lake level rise; Red: inversion uplift; Purple: compaction. The relative amount of effect on the accommodation space is indicated by size. Abbreviations; NS: Nagykanizsa subbasin; IH: Inke high; TS: Tarany subbasin; GBH: Görgeteg-Babócsa high.

Climatic-controlled lake level fluctuations

The sustained brackish water of Lake Pannon and its biostratigraphic evolution suggest that no communication existed with seawater and also it had no high discharge permanent outflow for much of the Late Miocene (Magyar and Sztanó, 2008). On the other hand, the inflow of large rivers originating from the surrounding orogens discharged water and sediments into the lake. Evaporation and precipitation then controlled the lake level fall or rise. However, this was also regulated by the size of the lake surface area, which as it shrunk cut back further lake level lowering.

43

Similar to previous studies (e.g. Uhrin and Sztanó, 2011) we conclude that decrease in foreset height is not directly linked to a climatic control. However, for the lake level rise, we find clear evidence of at least 7 episodes of major retrogradation (Fig. 19A&B). Based on the sensitivity interplay of local sedimentation rate and water level rise, such events can be manifested either in major retrogradation or aggradation of the overall prograding system.

The episodes of retrogradation did not cause a sudden drowning of the basin. Relating the phases of retrogradation (max ~100m, see Fig. 22f) to the rate of accommodation space creation (i.e. rapid relative lake level rise), during thermal subsidence, significantly exceeding the rate of sediment supply.

In contrast to previous studies here it is demonstrated that the interpreted and decompacted foreset heights are higher than the observations based on purely seismics (Fig. 25).
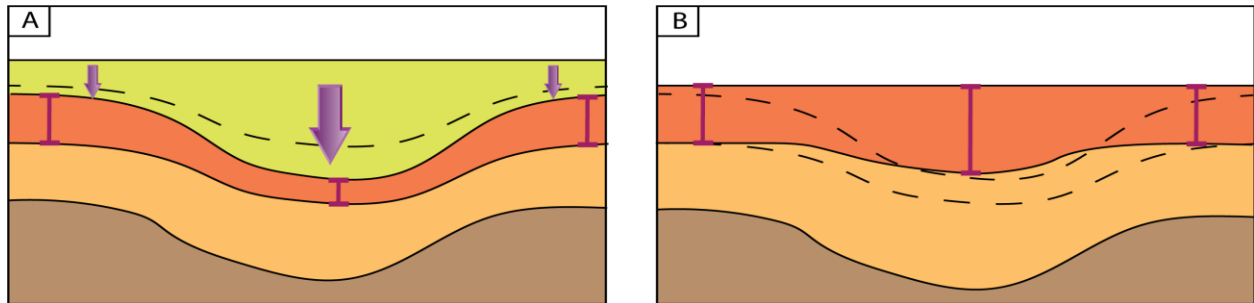
Figure 25: Illustration in increase of foreset height with incorporating the process of decompaction. The height of the decompacted foresets exceeds previously estimated average values of ~300 m. Without the process of decompaction estimating foreset heights is done without implementing forcing factors, and consequently difference in height is missed. A) Height of the foresets in the depth section. B) Height of the decompacted foresets after sequential reconstruction. Colors; Green: overlying load (shelf sed.); Red: compacted layer (foresets); Orange: underlying layer (bottomsets); Brown: Basement (pre-Pannonian).

Initial accommodation space related to the early Late Miocene paleo-relief

Early to Middle Miocene extension of the Pannonian Basin is characterized by accommodation of asymmetric (half-) grabens. The early Late Miocene inversion reversed Middle Miocene normal faults, resulting in pop-up structures. The resulting paleo-relief was featured by an alteration of highs and depressions (Figs. 19A&B and 22). The huge difference in initial accommodation space is found between depocenters and highs.

The process of sedimentation in confined basins is similar described by Sinclair and Tomasso, (2002). The progressive infill of confined basins divided by a geometric barrier can be characterized by four phases: (1) *Flow ponding*, where incoming flows are totally trapped, and depositing thick muddy sequences in the 'Trapping basin'. (2) *Flow stripping*, where the finer, more dilute portion of the flow can escape the trapping basin over de adjacent barrier into the starved basin. In the meantime, the trapping basin is totally filled as palaeobathymetries allow. (3) *Flow Bypassing the barrier*, where the trapping basin is sufficiently filled with sediment, and the barrier is predominantly buried. This leads to a bypass of the bulk of the sediment into the starved basin. (4) *Backfilling*, where the basins and the surrounding topography is completely blanketed, due to base-level rise.

Eventually at around 8.6 Ma the progradation reached the Nagykanizsa subbasin (trapping basin). The hummocky subparallel turbiditic seismic facies units fill the large available accommodation space, reaching up to 2000 m (Fig. 22f). On top the deposition of the clinoform seismic facies units of the prograding shelf-margin slope, and the fairly continuous sub-parallel seismic facies shelf sediments.

Finally, there was a decrease of the relief between basin and adjacent highs, caused by the accumulation of thick, sheet-like sand- stone lobes. This ended the effect of sediment ponding at the barrier, and gradually more turbidity currents were capable to overcome the highs and convey sedimentation to the next depocenter.

Bathymetries allowed the progradation covering the Inke high (barrier). However, the lack of accommodation space resulted in a thin turbiditic sequence with associated foresets and shelf sediments on top. Again accommodation space increased at the Tarany subbasin (starved basin), resulting in a thicker progradational sequence filling the subbasin. Reaching the Görgeteg-Babócsa high (new barrier) the lack of accommodation space caused a thinner prograding sequence comparable to the Inke high.
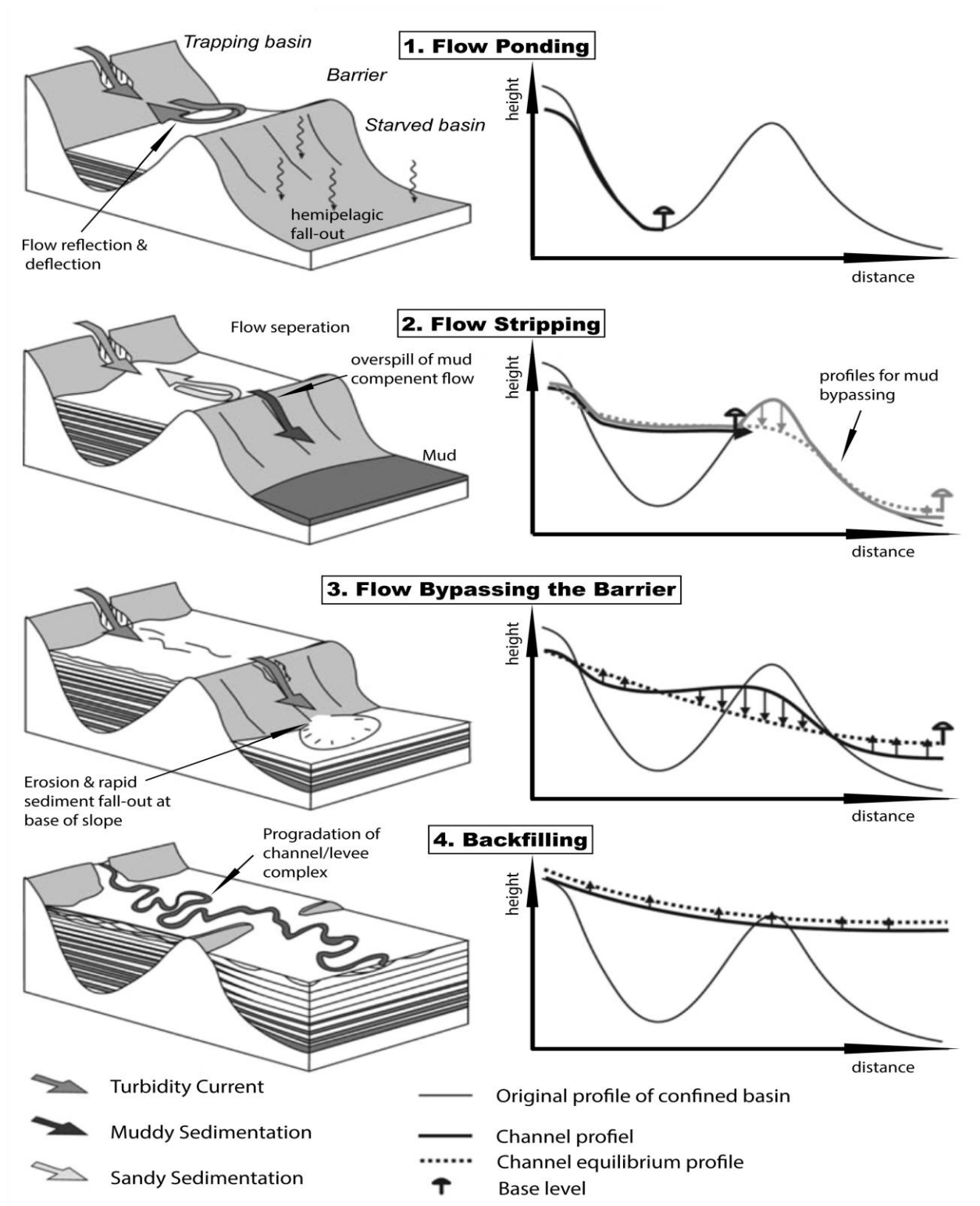
Figure 26: Schematic depositional model for the progressive infill of a confined basin and associated deposits at the base of the slope of a secondary 'starved basin' (modified after Sinclair & Tomasso, 2002). Moreover, the evolution of the actual and equilibrium profile of the channel is shown in the charts to the right. The four stages that can be identified: 1. Flow Ponding; Occurs when the trapping basin is surrounded by topographic barriers that are sufficient to prevent turbidity currents surmounting them; 2. Flow Stripping: Process of partial surmounting of the barrier by the uppermost, lower-density fraction of a turbidity current; 3. Flow Bypassing the Barrier: Occurs when the trapping basin is sufficiently filled with sediment, and the barrier is predominantly buried. This leads to a bypass of the bulk of the sediment into the starved basin; 4. Backfilling or Blanketing: The starved basin will be filled as much as available accommodation space and bathymetry allows.

46

Differential compaction and syn-sedimentary tectonics

As progradation is diachronous throughout the Pannonian Basin, an important process of syn-sedimentary compaction of pre-Late Miocene and early Late Miocene sediments, has significantly increased the accommodation space. Differential compaction occurred in this area, as a consequence of the existing paleo-relief and basement subsidence (Fig. 24C).

There is a large variation in thickness and compactibility of the different sequences in the Middle and Late Miocene in my study area. Especially, loading of early Late Miocene deposits on the Middle Miocene rift deposits caused a spatially variable amount of compaction. Not only the thickness of the load, but also the underlying structure has influence on the amount of compaction. This is similar to the description by Balázs (2016): 'The burial in late post-rift stage may create differential compaction effects over the half-grabens, such as synclinal geometries or compaction faults with increasing offsets towards the surface, in particular when the thickness of the overburden is high.'

The direct indicator of differential compaction in the area is given by the normal faults with increasing offset towards the top. The best example of this is found just above the Görgeteg-Babócsa high (Fig. 19B). Moreover, the strong folding of the prograding sequence is partly caused by the effects of differential compaction. Faults and folds in the post-rift sequence often form directly above the main fault as a result of the difference in compaction between the graben fill and the footwall (cf., ter Borgh, 2013).

Areas in which the differential compaction had a major influence lie in the footwall and hanging wall directly next to the inverted fault. The results showed that, in these so called intermediate areas; a relatively large thickness of the prograding body is present. This is directly linked to the influence of syn-sedimentary tectonics. The angular relationships between onlaps in foot -and hanging wall are commonly described to normal drag associated with syn-sedimentary faulting. This causes the early Late Miocene marls and turbiditic bodies to form synclinal drag structures along the inverted highs.

Loading is then strongly localized in the hinge of these synclinal structures, increasing the effect of compaction. Hence, locally increasing the accommodation space. The best example of this process is found to the north and south of the Görgeteg-Babócsa high (Fig.19B and Fig. 22b, data points 12 and 14).

The effect of differential compaction on the thickness variation in the prograding sequence of the Late Miocene is previously recognized by Balázs, (2016): 'Interesting is that the large-scale Pannonian progradation contains thicker prograding foresets above the former extensional basins, most likely due to differential compaction being active during deposition.'

Forcing factors as paleo-relief and differential compaction are directly influenced by syn-sedimentary tectonics like subsidence and uplift. The thermal subsidence originates from the start of the Late Miocene, enabling the Late Miocene to Quaternary sediments to reach up to several kilometres thickness. The subsidence increases the overall accommodation space available during deposition of the prograding sequence. Moreover, it increases the effect of syn-sedimentary compaction in the deeper parts. The best example of this is found in the Nagykanizsa subbasin (Fig. 24 and Fig. 22f, data point 2).

On the other hand, late inversion let to the uplift of reverse fault associated areas. This uplift counteracts the effect of subsidence primarily in the areas close to the inverted Middle-Miocene normal faults. Moreover, it creates drag structures as discussed previously.

The regional evolutionary model

The results showed that thermal subsidence in the area started early Late Miocene and proceeded, generating a vertical movement between 600 and 800 m (Fig. 22b-f). However, the subsidence had a differential character. The early to Late Miocene (Pannonian) extension was followed by highly variable amounts of post-rift thermal subsidence that spans from kilometres thick to no deposition and/or erosion (Matenco and Radivojevic, 2012). The differential subsidence of the basement led to the formation of several subbasins within the area of the lake (Uhrin and Sztanó, 2012). The Nagykanizsa - and Tarany are clear representations of these subbasins, located directly next to the major Zalá and Drava basins (for location, see Fig. 1 and 3).

Horvath et al., (2015) states: 'if compaction and sediment loading corrections are taken into account, one can arrive at about 600 m tectonic subsidence in the axial part of the Drava basin. This would mean that obtained results are relatively high compared to previous noted values. However, Horvath et al., (2015) related the amount of subsidence to seismic interpretation, whilst this study produced a reconstruction with decompaction and unfolding of young sediments. The overall thickness of Late Miocene to Quaternary sediments reaches up to several kilometres in the area. Reaching this thickness would mean that 600 to 800 m of subsidence is clearly possible.

Moreover, the area of interest is in the SW part of the basin and progradation only reached here at ~8.6 Ma, meaning that subsidence had reached significant amplitude. Areas of rapid uplift due to inversion were subjected to erosion and the eroded sediments progressively overfilled the generated accommodation space.

However, regional subsidence during Pliocene to Quaternary was still significant. An indication for this is the wedge of Pliocene to Quaternary sediments extending above the Tarany subbasin and the Görgeteg-Babócsa high. This wedge is thinning towards the north and diverting towards the south. Following this wedge more to the south is possible by looking at a cross-section (Fig. 6) made by Horváth et al., (2015). They interpreted that the Pliocene/Quaternary wedge is increasing into the Drava basin up to ~1.5 km depth (Fig. 6, 200 km).

For the characteristics of the Early Pliocene to recent inversion, we find that the vertical uplift within the cross-section varies between 80 m at the Inke high and up to 110 m at the Görgeteg-Babócsa high. This means that, comparable to the subsidence, the late inversion had a differential character. The amplitude of uplift is comparable with previous findings of Lenkey, (1999). He estimated the amount of erosion due to the inversional uplift to be 200-300 m, via comparison of porosity depth curves as mentioned in the methods and data chapter.

Moreover, the inversion led to high amplitude folding of Late Miocene to Quaternary sediments. The Pannonian Basin underwent a Pliocene-Quaternary reactivation, leading to large-scale warping of the lithosphere with a characteristic wavelength of several hundred kilometres (e.g. Cloetingh et al., 1999 and Vackarcs et al., 1994).

The link between late inversion tectonics and the paleo-water depth pattern

With the help of the illustration elaborating the forcing factors (Fig. 24C) I try to visualize the heterogeneity in both space and time. Linking this figure with results of the reconstruction (Fig. 22f and 23) and the observations done in tectono-sedimentary study (Fig. 19A&B), enables us to quantitatively define the influence of the different forcing factors.

The climatic forcing on the increase of the lake water level has a maximum of ~100 m along this section. The direct results for this are shown in the palaeobathymetric dataset with the 7 phases of retrogradation (Fig. 22f). Moreover, no evidence is found for a base level drop, resulting in an increase of water level from 8.6 till 6.8 Ma (Fig. 19A&B).

The maximum difference in height of the decompacted foresets of the Nagykanizsa subbasin and the Inke High is ~270 m (Fig. 23, data points 2/3 and 4). Looking at the forcing factors responsible for the difference (Fig. 24C); major influence of the initial accommodation space, the differential subsidence and the uplift due to inversion can be addressed.

This study confirms the importance of basement depth variations. For the Nagykanizsa subbasin and the Inke High this is max ~1500 m (Fig. 22f), however a big part of this is reduced by the deposition of the pelagic sedimentation at the start of the Late Miocene (Fig. 19A&B and 24C). These Endröd marls can reach up to approximately 1000-1300 m, when linking seismic facies (Fig. 22f) and onlaps at the Base Pannonian unconformity (Fig. 19A, ~18 km). The same can be done for the Tarany subbasin in comparison with the Görgeteg-Babócsa high as the difference in depth of the basement is ~500 m (Fig. 22f) and the thickness of the Endröd Fm reaches up to ~350 m (Fig 22f and Fig 19B, ~64 km). This means that the influence of the initial accommodation space (paleo-relief) on the height of the foresets is between ~150-200 m.

For subsidence the results showed (Fig. 22b-f) that the amount ranges between 600-800 m, this suggests that the influence of differential subsidence between depocenters and highs is max ~200 m. However, part of this is caused by the difference in syn-sedimentary compaction between the different geometric units. The amount of differential compaction can be addressed by looking at the difference in foreset height of the subbasins in the cross-section. Since, the foreset height difference in subbasins is mostly linked to difference in syn-sedimentary compaction (Fig. 24, NS and TS).

The difference in foreset height between the Nagykanizsa subbasin (Fig. 23, point 2) and the Tarany subbasin (Fig 23, point 8 and 9), is ~20-30 m. This means that the influence of tectonic differential vertical movements ranges between ~100-170 m and the influence of compaction is slightly lower.

The amount of uplift, which limits the height of the foresets on the paleo-highs, can be directly linked to the fault movement performed in the sequential reconstruction (Fig. 22b-f). As for the Inke high this was ~80 m and for the Görgeteg-Babócsa high ~110 m, resulting in an influence of uplift between ~80-110 m.

In the end the combination of all forcing factors, directly linked to the underlying geometry, results in the height of the foresets. The amplitude of the forcing factors changes in space and time (Fig 24C, see NS, IH, TS and GBH).

Implications for future research

Previous studies mostly focussed on dissecting the progradational infill of the Pannonian Basin solely on seismic and well data, followed by linking of the interpreted fluctuations in paleowater level by section flattening, to climatic forcing. However, similar to previous studies no real attention was given to time depth conversion and decompaction.

The proposed tectonic and sedimentary evolutionary model based on seismic and well data interpretation of the Pannonian Basin can be applied in similar inverted extensional basins as well. The model should firstly be expanded to 3D. Moreover, a correlation with previous studies, such as Sztanó et al., (2013), focusing on directional sediment infilling patterns is highly recommended.

Conclusions

The interpretation of seismic data from the Pannonian Basin in SW Hungary is calibrated with available well data and elaborated by a sequential reconstruction of a chosen cross-section. Focus was put on the interpretation of the shelf-margin slope sediments of the Algyö Formation and quantitatively linked to the late inversion structures along the cross-section. This has led to a novel image on the palaeobathymetry during Late Miocene shelf-margin slope progradation in Lake Pannon, as it was higher than previously estimated. For this study a regionally generalized porosity-depth curve is compiled using both: sand-shale ratios from available well data and previous established trends by Szalay, (1982). The resulting curve has proven to be representative for the area of interest. Moreover, a precise decompaction process has been applied in the reconstruction following Athy's relationship, incorporating the established porosity-depth curve. This was necessary to reconstruct the original palaeobathymetry during deposition.

The Late Miocene infill of Lake Pannon comprises of a prograding sequence with 4 different seismic facies. The topsets or shelf sediments from the Újfalu Fm. have a sub-parallel fairly continuous seismic facies. The foreset of the Algyö Fm. comprise of an alternation of continuous and discontinuous reflectors. Downslope, the bottomsets include two different seismic facies. Turbiditic bodies of the Szolnok Fm. drape the underlying marls of the Endröd Fm. The turbidites are characterized by hummocky discontinuous or a sub-parallel fairly reflectors, whilst the marls have a parallel sub-flat continuous seismic facies.

The reconstructed palaeobathymetric evolution varies within the cross-section from 150 to ca. 420 m. Variations in foreset height are directly linked to the geometry below. Moreover, it shows that between 8.6 and 6.8 Ma at least 7 phases of aggradation or retrogradation resulted in a maximum increase of water level of max ~100 m. Mostly, the palaeobathymetry slightly increased in periods of progradation. No indications are found for sudden drops of the water level below the shelf-edge. The decrease in foreset height is linked to changes in sedimentation and a limitation of accommodation space on the paleo-highs.
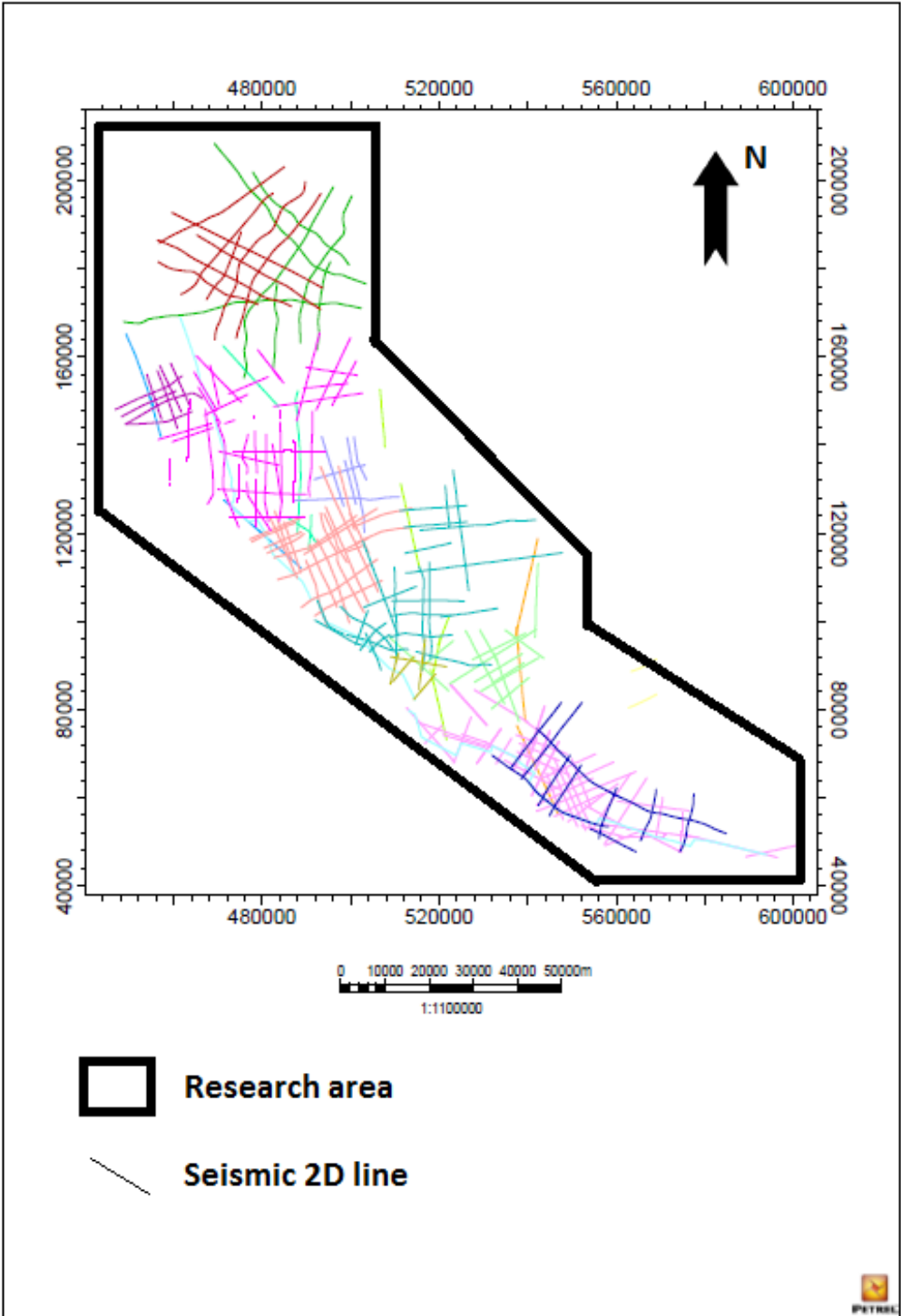
The influence of inversion tectonics on the Late Miocene prograding sequence varies in space and time. There are strong differences between depocenters, (Nagykanizsa -and Tarany subbasin) and highs (Inke - and Görgeteg-Babócsa high). However, the existing paleo-relief had the major effect on the available accommodation space at time of deposition. For the deep basins the influence of differential compaction and syn-sedimentary subsidence, increased the resulting accommodation space significantly. On the other hand, the highs suffered major uplift due to neotectonic inversion, leading to a further decrease of already limited initial accommodation space. The resulting palaeobathymetric evolution is a result of all these forcing factors combined at one place.

Acknowledgements

Appendix

Appendix A – Petrel Screenshot of the 2D seismic network

Appendix B – Seismic Mis-Tie Manager (Petrel)

		Use	🔒	Line/Cube	SP/ Plane	CDP/ Inline	Trace/ Xline	Vertical mis-tie	Correlation factor	Vertical correction	Vertical residual	Gain mis-tie	Gain correction	Intersecting
111		✓		Na-88_migr	1	141	141	63.52	0.7378	-11.92	75.44	0.00331	1.86165	D-1-F_migr
111		✓		Na-88_migr	1	60	60	79.72	0.8252	-11.92	91.64	0.01584	1.86165	H20_Amplitudes
111		✓		Na-88_migr	1	196	196	-0.44	0.8375	-11.92	11.48	2.34876	1.86165	na-63_migr
111		✓		Na-88_migr	1	232	232	-1.45	0.8389	-11.92	10.47	0.87407	1.86165	Na-82_migr
111		✓		Na-88_migr	1	294	294	-59.95	0.8480	-11.92	-48.03	1.09564	1.86165	Na-83_migr
112		✓		so-1_migr	1	12	12	-15.83	0.7763	-19.37	3.54	1.67118	5.76151	SO-81_migr
112		✓		so-1_migr	1	62	62	-7.47	0.7759	-19.37	11.90	5.57953	5.76151	so-82_migr
112		✓		so-1_migr	1	590	590	-286.50	0.6635	-19.37	-267.13	2.94525	5.76151	SO-5_migr
112		✓		so-1_migr	1	860	860	-7.30	0.7547	-19.37	12.08	0.84352	5.76151	na-61_migr
112		✓		so-1_migr	1	1163	1163	-17.96	0.7213	-19.37	1.41	5.24564	5.76151	na-60_migr
112		✓		DA-56_migr	1	560	560	0.84	0.8185	-8.03	8.86	0.36476	0.84974	SE_1_migr
112		✓		DA-56_migr	1	316	316	321.64	0.7771	-8.03	329.67	1.25300	0.84974	DA-24-A_migr - 2
112		✓		DA-56_migr	1	86	86	-28.37	0.7786	-8.03	-20.34	35702.36944	0.84974	da-30_stack_stack
112		✓		DA-56_migr	1	87	87	-57.38	0.7859	-8.03	-49.35	3.24417	0.84974	da-30_migr_migr
112		✓		DA-56_migr	1	568	568	19.41	0.8082	-8.03	27.44	1.09123	0.84974	DA-46_migr - 2

Appendix C – EOV settings for both Petrel and MOVE

HUN_EOV

Coordinate reference system (CRS)

Name:	HUN_EOV
Unit domain:	Projected
Description:	E_O_V

Authority code: Mammut,7000
Native surface unit: m

Extended WKT: PROJCS["Hungarian_1972_Egyseges_Orszagos_Vetuleti",GEOGCS["GCS_Hungarian_1972",DATUM ["D_Hungarian_1972",SPHEROID["GRS_1967",6378160.0,298.247167427]],PRIMEM["Greenwich",0.0],UNIT ["Degree",0.0174532925199433]],PROJECTION["Hotine_Oblique_Mercator_Azimuth_Center"],PARAMETER ["False_Easting",650000.0],PARAMETER["False_Northing",200000.0],PARAMETER ["Scale_Factor",0.99993],PARAMETER["Azimuth",90.0],PARAMETER ["Longitude_Of_Center",19.048571778],PARAMETER["Latitude_Of_Center",47.14439372222],UNIT["Meter",1.0]]

Reference CRS: GCS_Hungarian_1972

Textual CRS representation: ESRI: <?xml version="1.0" encoding="utf-16"?><IEarlyBoundCoordinateReferenceSystem

Area of use: Hungary.

Cartographic transform

Name:	Hungarian_1972_To_WGS_1984_2
From CRS:	GCS_Hungarian_1972

Authority code: EPSG,1831
To CRS: GCS_WGS_1984

Extended WKT: GEOGTRAN["Hungarian_1972_To_WGS_1984_2",GEOGCS["GCS_Hungarian_1972",DATUM ["D_Hungarian_1972",SPHEROID["GRS_1967",6378160.0,298.247167427]],PRIMEM["Greenwich",0.0],UNIT ["Degree",0.0174532925199433]],GEOGCS["GCS_WGS_1984",DATUM["D_WGS_1984",SPHEROID ["WGS_1984",6378137.0,298.257223563]],PRIMEM["Greenwich",0.0],UNIT["Degree",0.0174532925199433]],METHOD ["Geocentric_Translation"],PARAMETER["X_Axis_Translation",57.01],PARAMETER["Y_Axis_Translation",- 69.97],PARAMETER["Z_Axis_Translation",-9.29],AUTHORITY["EPSG",1831]]

✕ Close

Ascii Coordinate Transformation

Select a datum for the imported data. The data will be projected to the document coordinate system

● Datum and Projection ○ Standard Projections ○ US State Plane

Geographical Parameters

Datum:	EPSG
Name:	Hungarian_Datum_1972
EPSG code:	4237
Semi Major Axis	6378160.0 m
Semi Minor Axis	6356774.5 m
Inv Flattening	298.25
Prime Meridian	0.00 deg

Projection Parameters

Projection Type:	Hotine Oblique Mercator
Centre Latitude	47.14 deg
Centre Longitude	19.05 deg
Azimuth	90.00 deg
Rectified Grid Angle	90.00 deg
Scale Factor	0.9999
False Easting	650000.0 m
False Northing	200000.0 m

Show WKT>>>
Load From File...
Save To File...

Well known type

PROJCS[projection["Hotine_Oblique_Mercator"],GEOGCS["HD72",DATUM["Hungarian_Datum_1972",SPHEROID["GRS 1967",6378160,298.247167427,AUTHORITY["EPSG","7036"]],TOWGS84[52.17,-71.82,-14.9,0,0,0,0],AUTHORITY["EPSG","6237"]],PRIMEM["Greenwich",0,AUTHORITY["EPSG","8901"]],UNIT["degree",0.01745329 25199433,AUTHORITY["EPSG","9122"]],AUTHORITY["EPSG","4237"]],PARAMETER["latitude_of_center",47 .14439372222223],PARAMETER["longitude_of_center",19.04857177777778],PARAMETER["azimuth",90],PARAMETER["rectified_grid_angle",90],PARAMETER["scale_factor",0.99993],PARAMETER["false_easting",650000],PARAMETER["false_northing",200000]]

● Help   ☑ Show import summary   Cancel   Previous   Next

Appendix D – Base Pannonian unconformity depth surface
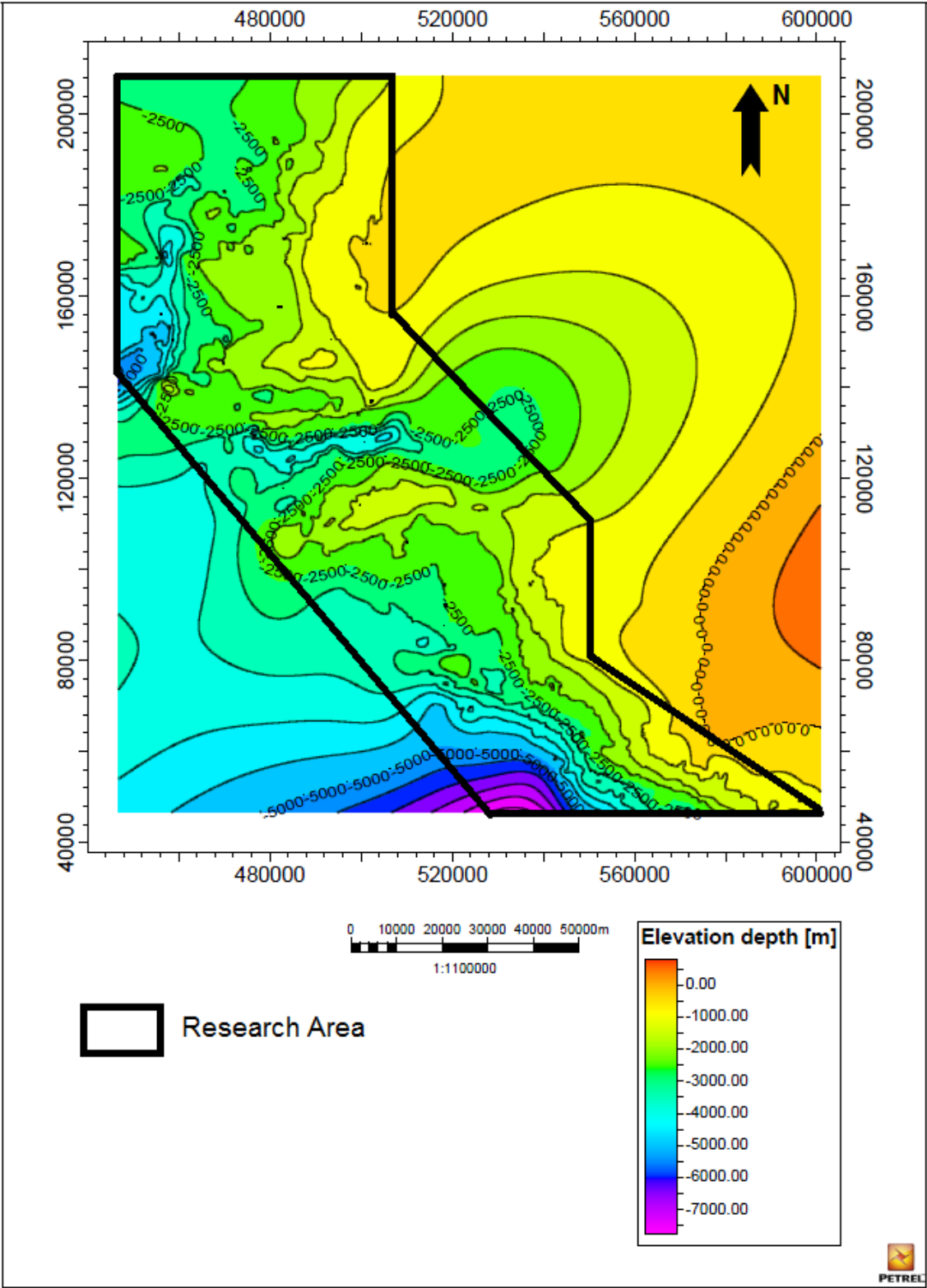
Appendix E – Shale/Sand ratio's enumerated per well

| Tarany-2					Gyenkenyes-1				
Top (m)	Bottom (m)	Shale	Sand	Ratio	Top (m)	Bottom (m)	Shale	Sand	Ratio
230	1488	0.22	0.78	0.29	230	800	0.30	0.70	0.43
1488	2628	0.80	0.20	4.00	800	1343	0.57	0.43	1.35
2628	2850	0.75	0.25	3.00	1343	2224	0.89	0.11	8.09
2850	2985	0.55	0.45	1.21	2224	2400	0.68	0.32	2.09
					2400	4652	0.15	0.85	0.18

Felsozzentmarton -1					Semjanhaza-3				
Top (m)	Bottom (m)	Shale	Sand	Ratio	Top (m)	Bottom (m)	Shale	Sand	Ratio
378	1598	0.34	0.66	0.52	40	1365	0.51	0.49	1.02
1598	2940	0.69	0.31	2.26	1365	2360	0.78	0.22	3.63
2940	3365	0.47	0.53	0.87	2360	2538	0.35	0.65	0.54
3365	3423	0.00	1.00	0.00	2538	2990	0.94	0.06	17.18
3423	3497	0.12	0.88	0.14	2990	3067	0.99	0.01	75.92

Appendix F – Trishear faulting (Erslev, 1991)
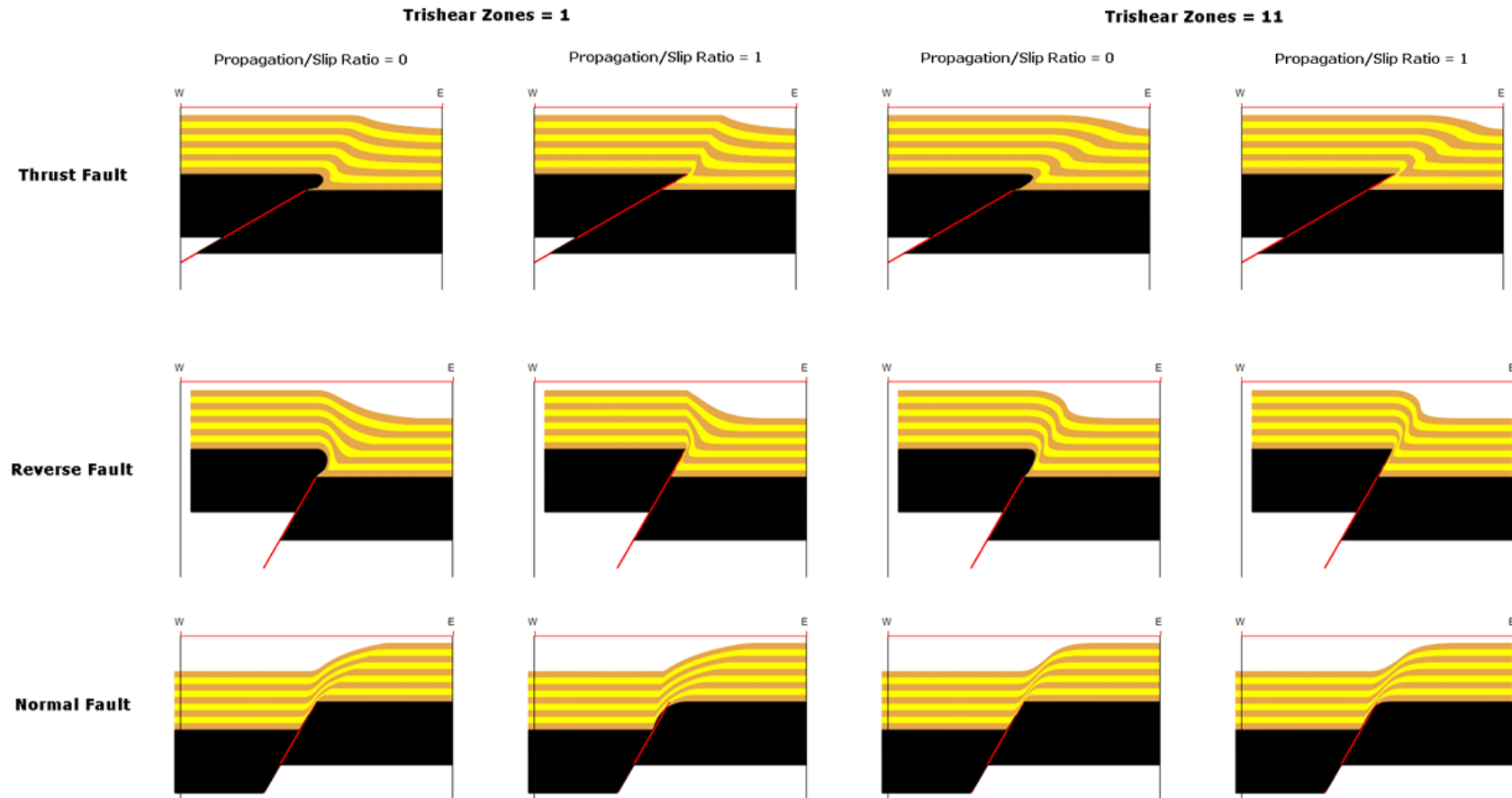
Bibliography

Bada, G., Horváth, F., Dövényi, P., Szafián, P., Windhoffer, G. & Cloetingh, S. 2007, "Present-day stress field and tectonic inversion in the Pannonian basin", *Global and Planetary Change,* vol. 58, no. 1, pp. 165-180.

Balázs, A., Matenco, L., Magyar, I., Horváth, F. & Cloetingh, S. 2016, "The link between tectonics and sedimentation in back-arc basins: New genetic constraints from the analysis of the Pannonian Basin", *Tectonics,* vol. 35, no. 6, pp. 1526-1559.

Baldwin, B. & Butler, C.O. 1985, "Compaction curves", *AAPG Bulletin,* vol. 69, no. 4, pp. 622-626.

Balla, Z. 1987, "Tertiary palaeomagnetic data for the Carpatho-Pannonian region in the light of Miocene rotation kinematics", *Tectonophysics,* vol. 139, no. 1-2, pp. 67-98.

Bishop, T.N. & Nunns, A.G. 1994, "Correcting amplitude, time, and phase mis-ties in seismic data", *Geophysics,* vol. 59, no. 6, pp. 946-953.

Catuneanu, O., Abreu, V., Bhattacharya, J., Blum, M., Dalrymple, R., Eriksson, P., Fielding, C.R., Fisher, W., Galloway, W. & Gibling, M. 2009, "Towards the standardization of sequence stratigraphy", *Earth-Science Reviews,* vol. 92, no. 1, pp. 1-33.

Cloetingh, S., Bada, G., Matenco, L., Lankreijer, A., Horváth, F. & Dinu, C. 2006, "Modes of basin (de) formation, lithospheric strength and vertical motions in the Pannonian-Carpathian system: inferences from thermo-mechanical modelling", *Geological Society, London, Memoirs,* vol. 32, no. 1, pp. 207-221.

Cloetingh, S., Burov, E. & Poliakov, A. 1999, "Lithosphere folding: Primary response to compression?(from central Asia to Paris basin)", *Tectonics,* vol. 18, no. 6, pp. 1064-1083.

Csato, I., Granjeon, D., Catuneanu, O. & Baum, G. 2013, "A three-dimensional stratigraphic model for the Messinian crisis in the Pannonian Basin, eastern Hungary", *Basin Research,* vol. 25, no. 2, pp. 121-148.

Csontos, L. & Nagymarosy, A. 1998, "The Mid-Hungarian line: a zone of repeated tectonic inversions", *Tectonophysics,* vol. 297, no. 1, pp. 51-71.

Erslev, E.A. 1991, "Trishear fault-propagation folding", *Geology,* vol. 19, no. 6, pp. 617-620.

Fodor, L., Bada, G., Csillag, G., Horváth, E., Ruszkiczay-Rüdiger, Z., Palotás, K., Síkhegyi, F., Timár, G., Cloetingh, S. & Horváth, F. 2005, "An outline of neotectonic structures and morphotectonics of the western and central Pannonian Basin", *Tectonophysics,* vol. 410, no. 1, pp. 15-41.

Handy, M.R., Ustaszewski, K., Kissling, E., Schmid, S.M. & Rosenberg, C.L. 2013, "" Wrong-way" subduction of South Alpine (Adriatic) lithosphere beneath the Eastern Alps-a kinematic appraisal", *EGU General Assembly Conference Abstracts*, pp. 11107.

Helland-Hansen, W. & Hampson, G. 2009, "Trajectory analysis: concepts and applications", *Basin Research,* vol. 21, no. 5, pp. 454-483.

Horváth, F., Musitz, B., Balázs, A., Végh, A., Uhrin, A., Nádor, A., Koroknai, B., Pap, N., Tóth, T. & Wórum, G. 2015, "Evolution of the Pannonian basin and its geothermal resources", *Geothermics,* vol. 53, pp. 328-352.

Horváth, F. 1995, "Phases of compression during the evolution of the Pannonian Basin and its bearing on hydrocarbon exploration", *Marine and Petroleum Geology,* vol. 12, no. 8, pp. 837-844.

Horváth, F., Bada, G., Szafián, P., Tari, G., Ádám, A. & Cloetingh, S. 2006, "Formation and deformation of the Pannonian Basin: constraints from observational data", *Geological Society, London, Memoirs,* vol. 32, no. 1, pp. 191-206.

Juhász, E., Phillips, L., Müller, P., Ricketts, B., Tóth-Makk, Á., Lantos, M. & Kovács, L. 1999, "Late Neogene sedimentary facies and sequences in the Pannonian Basin, Hungary", *Geological Society, London, Special Publications,* vol. 156, no. 1, pp. 335-356.

Juhász, G. 1991, "Lithostratigraphical and sedimentological framework of the Pannonian (sl) sedimentary sequence in the Hungarian Plain (Alföld), Eastern Hungary", *Acta Geologica Hungarica,* vol. 34, no. 1-2, pp. 53-72.

Juhász, G., Pogácsás, G., Magyar, I. & Vakarcs, G. 2007, "Tectonic versus climatic control on the evolution of fluvio-deltaic systems in a lake basin, Eastern Pannonian Basin", *Sedimentary Geology,* vol. 202, no. 1, pp. 72-95.

Krijgsman, W., Stoica, M., Vasiliev, I. & Popov, V. 2010, "Rise and fall of the Paratethys Sea during the Messinian Salinity Crisis", *Earth and Planetary Science Letters,* vol. 290, no. 1, pp. 183-191.

Lavier, L.L., Steckler, M.S. & Brigaud, F. 2000, "An improved method for reconstructing the stratigraphy and bathymetry of continental margins: Application to the Cenozoic tectonic and sedimentary history of the Congo margin", *AAPG Bulletin,* vol. 84, no. 7, pp. 923-939.

Leever, K.A., Matenco, L., Rabagia, T., Cloetingh, S., Krijgsman, W. & Stoica, M. 2010, "Messinian sea level fall in the Dacic Basin (Eastern Paratethys): palaeogeographical implications from seismic sequence stratigraphy", *Terra Nova,* vol. 22, no. 1, pp. 12-17.

Lenkey, L. 1999, *Geothermics of the Pannonian Basin and its bearing on the tectonics of basin evolution,* VU Department of Earth Sciences, PhD thesis, 212 pp., Amsterdam, Netherlands.

Magyar, I., Geary, D.H. & Müller, P. 1999, "Paleogeographic evolution of the Late Miocene Lake Pannon in Central Europe", *Palaeogeography, Palaeoclimatology, Palaeoecology,* vol. 147, no. 3, pp. 151-167.

Magyar, I., Radivojević, D., Sztanó, O., Synak, R., Ujszászi, K. & Pócsik, M. 2013, "Progradation of the paleo-Danube shelf margin across the Pannonian Basin during the Late Miocene and Early Pliocene", *Global and Planetary Change,* vol. 103, pp. 168-173.

Magyar, I. & Sztanó, O. 2008, "Is there a Messinian unconformity in the Central Paratethys", *Stratigraphy,* vol. 5, no. 3-4, pp. 245-255.

Márton, E. & Fodor, L. 2003, "Tertiary paleomagnetic results and structural analysis from the Transdanubian Range (Hungary): rotational disintegration of the Alcapa unit", *Tectonophysics,* vol. 363, no. 3, pp. 201-224.

Matenco, L. & Radivojević, D. 2012, "On the formation and evolution of the Pannonian Basin: Constraints derived from the structure of the junction area between the Carpathians and Dinarides", *Tectonics,* vol. 31, no. 6.

Matenco, L., Munteanu, I., Ter Borgh, M., Stanica, A., Tilita, M., Lericolais, G., Dinu, C. & Oaie, G. 2016, "The interplay between tectonics, sediment dynamics and gateways evolution in the Danube system from the Pannonian Basin to the western Black Sea", *Science of the Total Environment,* vol. 543, pp. 807-827.

Merten, S., Matenco, L., Foeken, J., Stuart, F. & Andriessen, P. 2010, "From nappe stacking to out-of-sequence postcollisional deformations: Cretaceous to Quaternary exhumation history of the SE Carpathians assessed by low-temperature thermochronology", *Tectonics,* vol. 29, no. 3.

Miall, A.D. & Miall, C.E. 2001, "Sequence stratigraphy as a scientific enterprise: the evolution and persistence of conflicting paradigms", *Earth-Science Reviews,* vol. 54, no. 4, pp. 321-348.

Nichols, G. 2009, "Subsurface Stratigraphy and Sedimentology & Sequence Stratigraphy and Sea-level changes" in *Sedimentology and stratigraphy*, Second edition, John Wiley & Sons, pp. 335-380.

Osborne, M.J. & Swarbrick, R.E. 1997, "Mechanisms for generating overpressure in sedimentary basins: a reevaluation", *AAPG Bulletin,* vol. 81, no. 6, pp. 1023-1041.

Ratschbacher, L., Frisch, W., Neubauer, F., Schmid, S. & Neugebauer, J. 1989, "Extension in compressional orogenic belts: the eastern Alps", *Geology,* vol. 17, no. 5, pp. 404-407.

Ratschbacher, L., Frisch, W., Linzer, H. & Merle, O. 1991, "Lateral extrusion in the Eastern Alps, part 2: structural analysis", *Tectonics,* vol. 10, no. 2, pp. 257-271.

Roberts, A., Yielding, G., Kusznir, N., Walker, I. & Dorn-Lopez, D. 1995, "Quantitative analysis of Triassic extension in the northern Viking Graben", *Journal of the Geological Society,* vol. 152, no. 1, pp. 15-26.

Rubey, W.W. & Hubbert, M.K. 1959, "Role of fluid pressure in mechanics of overthrust faulting II. Overthrust belt in geosynclinal area of western Wyoming in light of fluid-pressure hypothesis", *Geological Society of America Bulletin,* vol. 70, no. 2, pp. 167-206.

Saftić, B., Velić, J., Sztano, O., Juhasz, G. & Ivković, Ž. 2003, "Tertiary subsurface facies, source rocks and hydrocarbon reservoirs in the SW part of the Pannonian Basin (northern Croatia and south-western Hungary)", *Geologia Croatica,* vol. 56, no. 1, pp. 101-122.

Sangree, J. & Widmier, J. 1978, "Seismic stratigraphy and global changes of sea level, part 9: seismic interpretation of clastic depositional facies", *AAPG Bulletin,* vol. 62, no. 5, pp. 752-771.

Schmid, S.M., Bernoulli, D., Fügenschuh, B., Matenco, L., Schefer, S., Schuster, R., Tischler, M. & Ustaszewski, K. 2008, "The Alpine-Carpathian-Dinaridic orogenic system: correlation and evolution of tectonic units", *Swiss Journal of Geosciences,* vol. 101, no. 1, pp. 139-183.

Schmid, S.M., Scharf, A., Handy, M.R. & Rosenberg, C.L. 2013, "The Tauern Window (Eastern Alps, Austria): a new tectonic map, with cross-sections and a tectonometamorphic synthesis", *Swiss Journal of Geosciences,* vol. 106, no. 1, pp. 1-32.

Sclater, J.G. & Christie, P. 1980, "Continental stretching; an explanation of the post-Mid-Cretaceous subsidence of the central North Sea basin", *Journal of Geophysical Research,* vol. 85, no. B7, pp. 3711-3739.

Sinclair, H. & Tomasso, M. 2002, "Depositional evolution of confined turbidite basins", *Journal of Sedimentary Research,* vol. 72, no. 4, pp. 451-456.

Smallwood, J.R. 2002, "Use of V0-K depth conversion from shelf to deep-water: how deep is that brightspot?", *First Break,* vol. 20, no. 2.

Spencer, C.W., Szalay, Á. & Tatár, É. 1994, "Abnormal pressure and hydrocarbon migration in the Bekes basin" in *Basin Analysis in Petroleum Exploration* Springer, pp. 201-219.

Steckler, M.S., Mountain, G.S., Miller, K.G. & Christie-Blick, N. 1999, "Reconstruction of Tertiary progradation and clinoform development on the New Jersey passive margin by 2-D backstripping", *Marine Geology,* vol. 154, no. 1, pp. 399-420.

Szalay, A. 1982, "Possibilities of the reconstruction of basin evolution in the prediction of hydrocarbon prospects", *Hungarian Academy of Sciences, PhD thesis, 212 pp., Budapest, Hungary*.

Szalay, A. & Szentgyorgyi, K. 1988, "A Method for Lithogenetic Subdivision of Pannonian (sl) Sedimentary Rocks: Chapter 8", *AAPG Special Volumes,* pp. 89-96.

Sztanó, O., Sebe, K., Csillag, G. & Magyar, I. 2015, "Turbidites as indicators of paleotopography, Upper Miocene Lake Pannon, Western Mecsek Mountains (Hungary)", *Geologica Carpathica,* vol. 66, no. 4, pp. 331-344.

Sztanó, O., Szafián, P., Magyar, I., Horányi, A., Bada, G., Hughes, D.W., Hoyer, D.L. & Wallis, R.J. 2013, "Aggradation and progradation controlled clinothems and deep-water sand delivery model in the Neogene Lake Pannon, Makó Trough, Pannonian Basin, SE Hungary", *Global and Planetary Change,* vol. 103, pp. 149-167.

Tari, G., Dövényi, P., Dunkl, I., Horváth, F., Lenkey, L., Stefanescu, M., Szafián, P. & Tóth, T. 1999, "Lithospheric structure of the Pannonian basin derived from seismic, gravity and geothermal data", *Geological Society, London, Special Publications,* vol. 156, no. 1, pp. 215-250.

ter Borgh, M. 2013, "Connections between sedimentary basins during continental collision: how tectonic, surface and sedimentary processes shaped the Paratethys", *UU Department of Earth Sciences, PhD thesis, 212 pp., Utrecht, Netherlands*.

ter Borgh, M., Radivojević, D. & Matenco, L. 2015, "Constraining forcing factors and relative sea-level fluctuations in semi-enclosed basins: the Late Neogene demise of Lake Pannon", *Basin Research,* vol. 27, no. 6, pp. 681-695.

Timár, G. & Molnár, G. 2002, "A HD72→ ETRS89 transzformáció szabványosítási problémái (standardization problems of transformation)", *Eötvös Loránd Geophysical Department.*

Uhrin, A., Magyar, I. & Sztano, O. 2009, "Effect of basement deformation on the Pannonian sedimentation of the Zala Basin, SW Hungary", *Földtani Közlöny,* vol. 139, pp. 273-282.

Uhrin, A. & Sztanó, O. 2012, "Water-level changes and their effect on deepwater sand accumulation in a lacustrine system: a case study from the Late Miocene of western Pannonian Basin, Hungary", *International Journal of Earth Sciences,* vol. 101, no. 5, pp. 1427-1440.

Ustaszewski, K., Schmid, S.M., Fügenschuh, B., Tischler, M., Kissling, E. & Spakman, W. 2008, "A map-view restoration of the Alpine-Carpathian-Dinaridic system for the Early Miocene", *Swiss Journal of Geosciences,* vol. 101, no. 1, pp. 273-294.

Vakarcs, G., Vail, P., Tari, G., Pogácsás, G., Mattick, R. & Szabó, A. 1994, "Third-order Middle Miocene-Early Pliocene depositional sequences in the prograding delta complex of the Pannonian Basin", *Tectonophysics,* vol. 240, no. 1-4, pp. 81-106.

van Hinsbergen, D.J., Dupont-Nivet, G., Nakov, R., Oud, K. & Panaiotu, C. 2008, "No significant post-Eocene rotation of the Moesian Platform and Rhodope (Bulgaria): implications for the kinematic evolution of the Carpathian and Aegean arcs", *Earth and Planetary Science Letters,* vol. 273, no. 3, pp. 345-358.